The Plant Cell, Vol. 27: 1755–1770, June 2015, www.plantcell.org

Wheat Stripe Rust Resistance Protein WKS1 Reduces the Ability of the Thylakoid-Associated Ascorbate Peroxidase to Detoxify Reactive Oxygen Species[OPEN]

Jin-Ying Gou,[a,b] Kun Li,[a,c] Kati Wu,[a] Xiaodong Wang,[a] Huiqiong Lin,[a] Dario Cantu,[d] Cristobal Uauy,[e,f] Albor Dobon-Alonso,[e] Takamufi Midorikawa,[a] Kentaro Inoue,[a] Juan Sánchez,[a] Daolin Fu,[c] Ann Blechl,[g] Emma Wallington,[f] Tzion Fahima,[h] Madhu Meeta,[i] Lynn Epstein,[j] and Jorge Dubcovsky[a,k,1]

[a] Department of Plant Sciences, University of California, Davis, California 95616
[b] State Key Laboratory of Genetic Engineering, Institute of Plant Biology, School of Life Sciences, Fudan University, Shanghai 200433, China
[c] State Key Laboratory of Crop Biology, Shandong Agricultural University, Tai'an, Shandong 271018, China
[d] Department of Viticulture and Enology, University of California, Davis, California 95616
[e] John Innes Centre, Norwich Research Park, Norwich NR4 7UH, United Kingdom
[f] National Institute of Agricultural Botany, Cambridge CB3 0LE, United Kingdom
[g] U.S. Department of Agriculture-Agricultural Research Service, Western Regional Research Center, Albany, California 94710
[h] Institute of Evolution and the Department of Evolutionary and Environmental Biology, University of Haifa, Haifa 31905, Israel
[i] Department of Plant Breeding and Genetics, Punjab Agricultural University, Ludhiana 141004, Punjab, India
[j] Department of Plant Pathology, University of California, Davis, California 95616
[k] Howard Hughes Medical Institute, Chevy Chase, Maryland 20815

ORCID IDs: 0000-0002-9814-1770 (C.U.); 0000-0002-7571-4345 (J.D.)

Stripe rust is a devastating fungal disease of wheat caused by *Puccinia striiformis* f. sp *tritici* (*Pst*). The *WHEAT KINASE START1* (*WKS1*) resistance gene has an unusual combination of serine/threonine kinase and START lipid binding domains and confers partial resistance to *Pst*. Here, we show that wheat (*Triticum aestivum*) plants transformed with the complete *WKS1* (variant *WKS1.1*) are resistant to *Pst*, whereas those transformed with an alternative splice variant with a truncated START domain (*WKS1.2*) are susceptible. WKS1.1 and WKS1.2 preferentially bind to the same lipids (phosphatidic acid and phosphatidylinositol phosphates) but differ in their protein-protein interactions. WKS1.1 is targeted to the chloroplast where it phosphorylates the thylakoid-associated ascorbate peroxidase (tAPX) and reduces its ability to detoxify peroxides. Increased expression of *WKS1.1* in transgenic wheat accelerates leaf senescence in the absence of *Pst*. Based on these results, we propose that the phosphorylation of tAPX by WKS1.1 reduces the ability of the cells to detoxify reactive oxygen species and contributes to cell death. This response takes several days longer than typical hypersensitive cell death responses, thus allowing the limited pathogen growth and restricted sporulation that is characteristic of the *WKS1* partial resistance response to *Pst*.

INTRODUCTION

Wheat (*Triticum aestivum* and *Triticum turgidum*) provides roughly 20% of the calories and 25% of the protein consumed worldwide (http://faostat3.fao.org/). Although more than 700 million tons of wheat are produced per year, further increases are required to match the demand of a continuously growing human population. One avenue to increase wheat production is to reduce losses caused by wheat pathogens. Among these, *Puccinia striiformis* f. sp *tritici* (*Pst*), the causal agent of wheat stripe rust (also known as yellow rust), is responsible for major yield losses in most wheat-producing areas. Recent worldwide epidemics are associated with the emergence of new virulent and highly aggressive *Pst* races that are now found at high frequencies on five continents (Milus et al., 2009; Hovmøller et al., 2010). The most effective and environmentally friendly strategy to limit yield losses caused by *Pst* has been the deployment of resistance genes, which for yellow rust are known as *Yr* genes (McIntosh et al., 2013; Maccaferri et al., 2015).

Wheat rust resistance genes are divided into two general categories: race-specific and race nonspecific (Lowe et al., 2011). Most race-specific resistance genes encode NB-LRR proteins, which include a nucleotide binding (NB) site domain and a leucine-rich repeat (LRR) (Michelmore et al., 2013). These genes, referred to hereafter as *R* genes, detect the presence of specific races of the pathogen and initiate a hypersensitive reaction (Spoel and Dong, 2012). Hypersensitive reactions are characterized by the fast accumulation of reactive oxygen species (ROS) (Torres, 2010) and a rapid programmed cell death of the infected cells, which limits further pathogen colonization of the host (Coll et al., 2011). By contrast, the molecular mechanisms involved in race nonspecific resistance genes are still poorly understood. In the wheat-rust pathosystem, this type of resistance is usually associated with a "slow rusting" or "partial resistance" phenotype because the pathogen is able to

[1] Address correspondence to jdubcovsky@ucdavis.edu.
The author responsible for distribution of materials integral to the findings presented in this article in accordance with the policy described in the Instructions for Authors (www.plantcell.org) is: Jorge Dubcovsky (jdubcovsky@ucdavis.edu).
[OPEN]Articles can be viewed online without a subscription.
www.plantcell.org/cgi/doi/10.1105/tpc.114.134296

establish itself, but is restricted in its growth and sporulation. Only two race nonspecific resistance genes against the wheat rusts have been identified so far (Fu et al., 2009; Krattinger et al., 2009), and their resistance mechanisms have been unclear.

One of these partial resistance genes is *Yr36*, which was cloned from wild tetraploid wheat (*T. turgidum* ssp *dicoccoides*) (Fu et al., 2009). *Yr36* encodes a protein designated as WHEAT KINASE START1 (WKS1) that is composed of a serine/threonine kinase domain and a steroidogenic acute regulatory protein-related lipid transfer (START) domain (Fu et al., 2009). The WKS1 kinase present in the N-terminal region is a functional non-arginine-aspartate (non-RD) kinase (Fu et al., 2009). The START domain in the C-terminal region of WKS1 is most similar to the START domain in *Arabidopsis thaliana* ENHANCED DISEASE RESISTANCE2 **(**EDR2), a protein that negatively regulates plant defense to the powdery mildew pathogen *Golovinomyces cichoracearum* (Tang et al., 2005; Vorwerk et al., 2007). START domains are characterized by a hydrophobic ligand binding pocket and are involved in lipid/sterol binding, transport, and signaling in both animal and plant species (Schrick et al., 2014), but the lipid ligands for the START domains present in WKS1 and EDR2 have not yet been characterized.

Single amino acid substitutions in either the START or the kinase domain result in susceptible phenotypes, indicating that both domains are required for *Pst* resistance (Fu et al., 2009). Two major alternative splice variants of *WKS1* have been detected: *WKS1.1*, which encodes the complete protein, and *WKS1.2*, which encodes a protein with a START domain truncated at the C terminus as a result of the exclusion of exon 11 (Figure 1A). Our previous study has shown that the transcript levels of *WKS1.1* relative to *WKS1.2* increase during the first days of *Pst* infection and at higher temperatures (Fu et al., 2009). In this study, we establish that *WKS1.1* (but not *WKS1.2*) confers resistance to *Pst* in wheat (*T. aestivum*) and advance our understanding of the molecular mechanisms associated with WKS1.1 partial resistance to *Pst*.

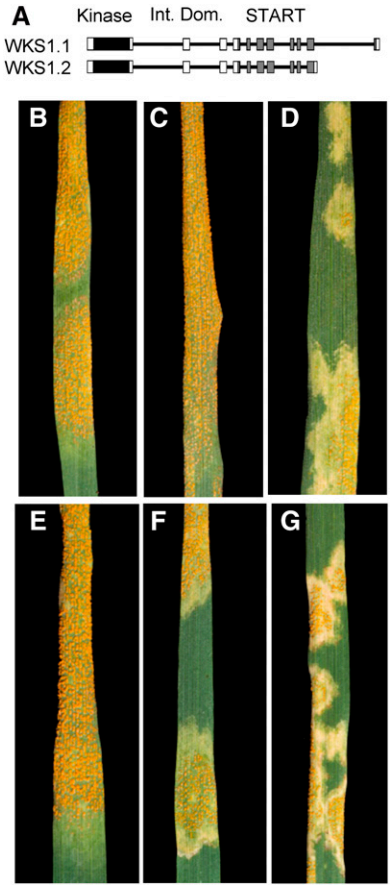

Figure 1. Wheat Plants Transformed with NP:WKS1.1 and NP:WKS1.2 and Inoculated with *Pst* Race PST-08/21.

(A) Schematic representation of *WKS1.1* and *WKS1.2* genes. Introns are represented by black lines and exons by boxes: black = kinase domain, white = inter domain, and gray = START domain.
(B) to **(G)** Stripe rust infection severity in plants inoculated with PST-08/21 15 dpi.
(B) Susceptible control Glasgow.
(C) Susceptible control UC1041.
(D) Resistant control UC1041+*WKS1*.
(E) Glasgow transformed with NP:WKS1.2. NP, native promoter.
(F) and **(G)** Two independent transformation events with NP:WKS1.1.

RESULTS

WKS1 Resistance Response against *Pst* Takes Several Days Longer Than Typical Hypersensitive Responses

To understand better the dynamics of the *Pst* infection in the presence and absence of *WKS1*, we characterized pathogen growth and development in the interveinal regions of leaves in three pairs of hexaploid wheat isogenic lines (UC1041 with and without *WKS1* and two pairs of sister lines each with and without a loss-of-function mutation in the *WKS1* kinase domain; Fu et al., 2009). To visualize the fungus, segments of leaves were stained with Uvitex 2B (Polysciences). During the first 6 d post-inoculation (dpi), we detected no significant differences in fungal development between the lines with and without *WKS1* (Supplemental Figure 1). In the second week after inoculation, the susceptible control lines showed a significantly higher percentage of interveinal zones with advanced pathogen networks than the isogenic lines with a functional *WKS1* (10 and 13 dpi; Supplemental Figure 1). The differential resistance response of lines with and without *WKS1* at the different time points resulted in a significant interaction between genotype and time after inoculation (two-way factorial ANOVA, $P < 0.0001$). In summary, the progression of WKS1-based resistance response to *Pst* described here takes several days longer than typical wheat hypersensitive reaction responses to *Pst* described in previous studies, which show necrotic cells within 2 to 4 dpi (Wang et al., 2007).

Alternative Splice Variant *WKS1.1*, but Not *WKS1.2*, Confers Resistance to *Pst*

To investigate the roles of *WKS1* alternative splice variants (Figure 1A) in *Pst* resistance, we transformed the susceptible hexaploid wheat variety Glasgow with constructs including

WKS1.1 and *WKS1.2* coding regions under the control of the native promoter (Table 1, NP:WKS1.1 and NP:WKS1.2). We then used *Pst* race PST-08/21 (Cantu et al., 2013) to inoculate transgenic plants expressing each alternative splice variant, as well as nontransgenic control plants and isogenic hexaploid wheat lines with and without the wild-type *WKS1* gene (UC1041+*WKS1* and UC1041, respectively) (Fu et al., 2009). All six independent transgenic events carrying NP:WKS1.2 were as susceptible to *Pst* as Glasgow and UC1041 susceptible controls (Figures 1B, 1C, and 1E). By contrast, all five transgenic wheat lines carrying the alternative splice variant NP:WKS1.1 were resistant to PST-08/21 (Figures 1F and 1G) and showed the characteristic partial resistance response observed in the resistant control UC1041+*WKS1* (Figure 1D). For each transgenic event, we calculated the average resistance and SE using 5 to 10 plants per event (Supplemental Table 1). Representative pictures of the *Pst* reactions for each transgenic event are provided in Supplemental Figure 2. To investigate possible causes of the different resistance responses of WKS1.1 and WKS1.2, we analyzed their lipid binding profiles, their ability to form homodimers, and their ability to interact with other proteins.

WKS1.1 and WKS1.2 Have Similar Lipid Binding Profiles

In vitro lipid binding assays were used to assess the ability of full-length proteins WKS1.1 and WKS1.2 to bind to membrane lipids and to test if the binding was mediated by the START domain. In the first experiment, we tested 15 different membrane lipids that were immobilized onto a nitrocellulose membrane (Figure 2A). Using polyclonal antibodies raised against glutathione *S*-transferase (GST), we found that both GST-WKS1.1 and GST-WKS1.2 proteins (produced by wheat germ in vitro translation) had clear affinities for phosphatidic acid (PA) and for mono-, di-, and triphosphorylated forms of phosphatidylinositol phosphates (PIPs; Figure 2A). No affinity was detected for the nonphosphorylated form of phosphatidylinositol (PI) or for the other 10 membrane lipids present in this blot (Figure 2A). A separate experiment using the START domain of WKS1.1 (GST-START) showed the same result (Figure 2A).

Based on this result, we selected a more specific lipid blot including PI and seven PIPs at different concentrations. This experiment confirmed the affinity of both WKS1.1 and WKS1.2 to mono-, di-, and triphosphorylated forms of PI and their lack of affinity for nonphosphorylated PI (Figure 2B). The interactions with $PI(3,4)P_2$ and $PI(3,4,5)P_3$ are not biologically relevant because these PIPs have not been found in plants (Munnik and Vermeer, 2010). Hybridization of the same lipid blot with GST-START domains from both WKS1.1 and WKS1.2 showed similar profiles to those obtained from the full-length proteins (Figure 2B). The START domains alone exhibited similar profiles to one another but a relatively weaker affinity for the monophosphorylated forms of phosphatidylinositol than their respective full-length proteins (Figure 2B). Taken together, these results indicate that the lipid binding ability of the full-length WKS1 protein is most likely mediated by the START domains and that WKS1.1 and WKS1.2 have similar lipid binding affinities.

WKS1.1 and WKS1.2 Differ in Their Ability to Form Homodimers

We used a yeast two-hybrid (Y2H) assay to test the ability of WKS1.1 and WKS1.2 proteins to form homodimers. Primers for the different Y2H constructs are described in Supplemental Table 2. We first confirmed that no construct shows autoactivation when tested against an empty bait or prey vector (e.g., WKS1.1 shown in Figure 3B). The full-length WKS1.1 protein formed homodimers on yeast minimal media/synthetic defined medium (SD) lacking leucine, tryptophan, and histidine (SD -L -W -H) even at the 1:500 dilution (Figures 3C and 3D), but no interaction was detected in the more stringent SD medium lacking also adenine (SD -L -W -H -A; Figures 3C and 3D). By contrast, homodimers were not detected for WKS1.2, even in the less stringent SD -L -W -H medium (Figure 3D). Weak interactions were detected between WKS1.1 and WKS1.2 proteins (Figure 3C).

To determine the WKS1.1 regions responsible for the protein-protein interactions, we subcloned the kinase domain alone (KA), the kinase with the interdomain region (KI), the START domain

Table 1. Transgenic Wheat Plants Used in This Study

Construct	Target Gene	Vector Backbone	Promoter	Transformation Method	Bact. Selection[a]	Plant Selection	Host Variety	Purpose
NP:WKS1.1	*WKS1.1*	pRLF10	Native WKS1[b]	Agro	amp 100, kan 20	G418	*T. aestivum* Glasgow	Function of transcript variant
NP:WKS1.2	*WKS1.2*	pRLF10	Native WKS1[b]	Agro	amp 100, kan 20	G418	*T. aestivum* Glasgow	Function of transcript variant
Ubi:TAP-WKS1.1	*WKS1.1*	pCAMBia1300[c]	Maize Ubi	Bombardment	kan 50	Bialaphos	*T. aestivum* Bobwhite	CoIP
NP:WKS1.1-GFP	*WKS1.1*	pGWB4[d]	Native WKS1[b]	Bombardment	kan 50	Bialaphos	*T. aestivum* Bobwhite	Subcellular localization
NP:GFP	*GFP*	pGWB4[d]	Native WKS1[b]	Bombardment	kan 50	Bialaphos	*T. aestivum* Bobwhite	Subcellular localization control

[a]amp, ampicillin; kan, kanamycin.
[b]Native WKS1 promoter includes 3543 bp upstream from starting codon.
[c]Rohila et al. (2006).
[d]Nakagawa et al. (2007).

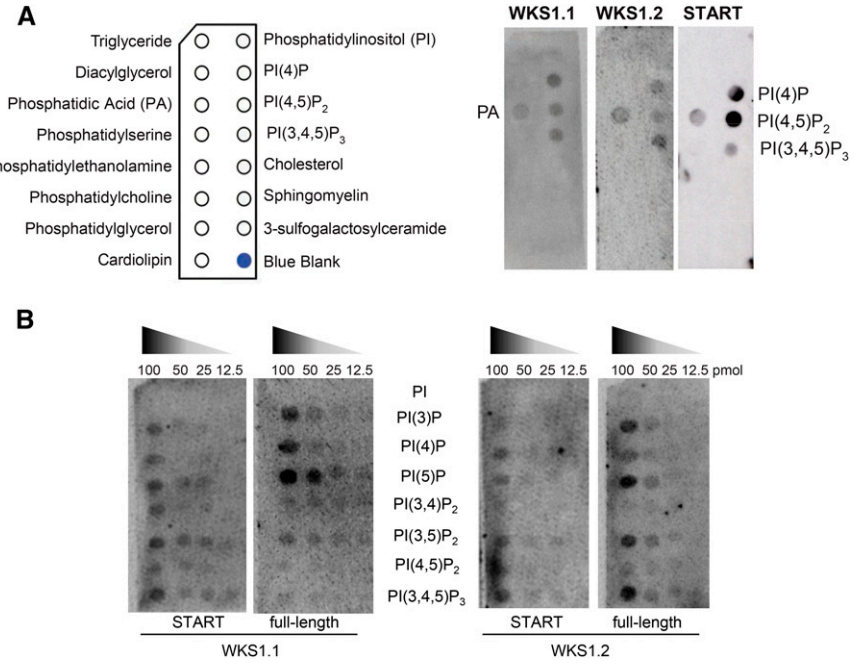

Figure 2. Binding of GST-Tagged WKS1.1 and WKS1.2 Proteins and Their Respective START Domains to Lipid Blots.

(A) Lipid blot with general membrane lipids. The schematic panel to the left indicates the positions of different lipids in the membrane. Membranes hybridized with GST-WKS1.1, GST-WKS1.2, and GST-START domain (from WKS1.1).
(B) Lipid blot with decreasing concentrations of PI and other PIPs evaluated with full-length GST-WKS1.1 and GST-WKS1.2 proteins and their corresponding GST-START domains.

alone (SA), and the interdomain region with the START domain (IS) (Figure 3A). Proteins encoded by the KA and KI constructs interacted with the full-length WKS1.1 (Figure 3C) and formed homodimers in both selection media (Figure 3D). The peptide including the START domain alone was not able to interact with the full-length WKS1.1 and was unable to form homodimers (Figures 3C and 3D). By contrast, the protein including the interdomain and the START domain (IS) was able to interact with WKS1.1 and to form homodimers in both selection media (Figures 3C and 3D). Based on these results, we concluded that the kinase domain is sufficient for dimerization and that the presence of the interdomain region enhances the formation of homodimers.

We also studied the effect on dimerization of four mutations in the kinase domain (wks1a-d) and one in the START domain (wks1e) of WKS1.1 (Supplemental Figure 3A) that result in complete *Pst* susceptibility (Fu et al., 2009). Mutations *wks1a* and *wks1b* had small effects on the interactions with the full-length wild-type WKS1.1, but showed noticeable reductions in their ability to form homodimers (Supplemental Figures 3B to 3D). By contrast, kinase mutations *wks1c* and *wks1d* significantly reduced the ability of the mutant protein to interact with the wild-type WKS1.1, and mutant homodimers were not detected (Supplemental Figures 3B to 3D). The *wks1e* mutation in the START domain showed an interaction profile similar to that observed for the *wsk1c* and *wks1d* kinase mutations (Supplemental Figure 3E). Based on these results, we concluded that all five loss-of-function mutations either reduce or eliminate the ability of WKS1.1 to form homodimers.

WKS1.1 and WKS1.2 Differ in Their Ability to Bind Interacting Proteins

The screening of a Y2H cDNA library from *Pst* infected leaves of tetraploid wheat (Yang et al., 2013) using both full-length WKS1 and kinase interdomain (KI) constructs as bait yielded 16 positive clones under stringent (SD -L -W -H -A) selection. Ten of these clones showed autoactivation and were discarded. Among the remaining six clones, three encoded a wheat thylakoid-associated ascorbate peroxidase (Danna et al., 2003) (henceforth, tAPX), two encoded a vesicle-associated protein 1-3-like (henceforth, VAP1-3), and one encoded an inositol hexakisphosphate and diphosphoinositol-pentakisphosphate kinase 1-like protein (henceforth, PPIP5K1-like) (Supplemental Table 3). For tAPX and VAP1-3, we cloned the full-length coding regions from diploid wheat *Triticum monococcum* and used them to validate the Y2H interactions with WKS1.1 (Supplemental Figure 4 and Supplemental Table 3). The WKS1 interaction with PPIP5K1-like was validated with the original positive clone found in theY2H screen, which includes only the last three exons of the coding region (Supplemental Figure 4 and Supplemental Table 3).

The three interactors detected in the Y2H screen were also tested for interactions with WKS1.2, the partial KI protein, and the five wks1a-e mutants (Supplemental Figure 4 and Supplemental Table 3). All three proteins interacted with KI and WKS1.1, confirming the results from the original screening and the importance of the kinase in these interactions. The interactions of tAPX and VAP1-3 with KI were stronger than those with the complete

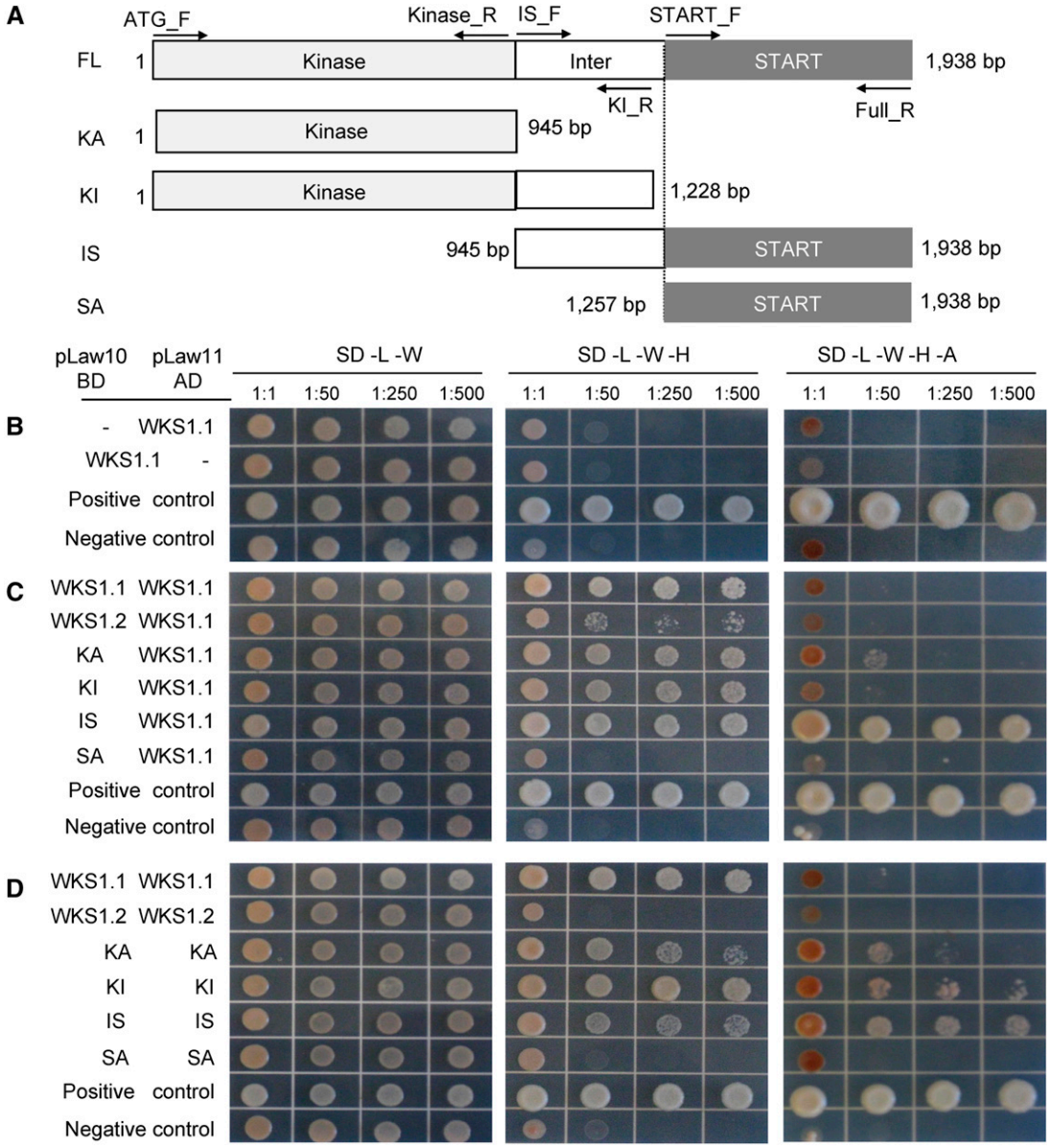

Figure 3. Homodimerization of WKS1.1 and WKS1.2 in Y2H Assays Using Complete and Partial Protein Segments.

(A) Protein regions used in Y2H assays: full-length (FL), kinase domain alone (KA), kinase with interdomain (KI), interdomain with START domain (IS), and START domain alone (SA). Primers are indicated by horizontal arrows and listed in Supplemental Table 2.
(B) WKS1.1 autoactivation test. BD, binding domain; AD, activation domain.
(C) Interaction between complete WKS1.1 and complete WKS1.2 or truncated WKS1 proteins.
(D) Homodimerization of WKS1 domains.
(B) to **(D)** Positive control = pGBKT7-53/pGADT7-T; negative control = pLAW10/pLAW11. See Supplemental Figure 3 for mutants and Supplemental Figure 5 for control protein gel blots.

WKS1.1 protein. None of the three proteins identified in the Y2H screen were able to interact with WKS1.2 or with the mutant proteins wks1c, wks1d, or wks1e (Supplemental Figure 4 and Supplemental Table 3). Protein gel blot analysis confirmed that WKS1.2 and mutant wks1 proteins were not degraded in the Y2H assays showing no positive interactions (Supplemental Figure 5). However, a lower level of protein was observed for WKS1.2 and mutant WKS1.1c (Supplemental Figure 5), which may have contributed to the failure to detect positive interactions. Mutant proteins wks1a and wks1b exhibited detectable interactions with tAPX, VAP1-3, and PPIP5K1-like, but they were weaker than with wild-type WKS1. The only exception was the PPIP5K1-like

interaction with wks1b, which was as strong as the interaction with the wild-type WKS1. These interactions parallel the results from the homodimerization tests (Supplemental Figure 3), suggesting that the formation of WKS1.1 homodimers may favor the interactions between WKS1.1 with tAPX, VAP1-3, and PPIP5K1-like proteins.

The Y2H interaction between tAPX and WKS1.1 was validated using a bimolecular fluorescence complementation assay in *Nicotiana benthamiana* (Supplemental Figure 6). Cells from *N. benthamiana* epidermal layer have very few or no chloroplasts so the observed cytoplasmic localization is not unexpected. In addition, the fusion of YFP (yellow fluorescent protein) to the N-terminal region of tAPX may have also interfered with its chloroplast localization signal. The interaction between tAPX and WKS1.1 was further validated in wheat plants by coimmunoprecipitation (CoIP) (Figure 4). Using a commercial rabbit tAPX antibody, we detected a specific band of ~40 kD in pull-down samples from the transgenic plants overexpressing TAP-WKS1.1, but not in those from the nontransgenic control (Figure 4). The size of this band corresponds with the expected size of a mature wheat tAPX protein (40.2 kD). This last experiment confirmed that the interaction between WKS1.1 and tAPX detected in yeast and in *N. benthamiana* also occurs in wheat plants. Since tAPX is a well-characterized chloroplast protein (Shigeoka et al., 2002), this result suggests that WKS1.1 has a chloroplast localization.

WKS1.1 Is Targeted to Chloroplasts

To determine the subcellular localization of WKS1.1 in wheat cells in vivo, we generated stable transgenic wheat plants expressing the coding sequence of WKS1.1 fused with the green fluorescent protein (GFP) under the control of the *WKS1* native promoter (NP:WKS1.1-GFP). As a negative control, we also generated stable transgenic plants expressing GFP alone under the control of the same promoter (NP:GFP) (Table 1). As expected, no GFP fluorescence was observed in the nontransgenic Bobwhite (Figure 5A), and fluorescence was detected in the cytoplasm in the NP:GFP transgene control (Figure 5B). In two independent transgenic lines expressing the WKS1.1-GFP fusion protein, fluorescence was detected in the chloroplasts of mesophyll cells where it colocalized with chlorophyll autofluorescence (Figures 5C and 5D).

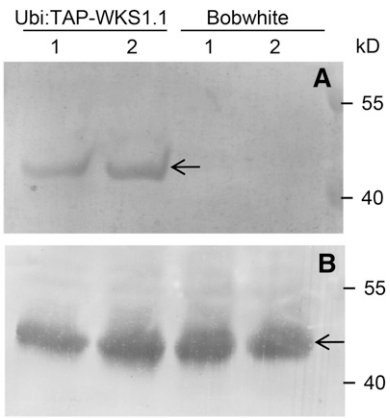

Figure 4. In Planta Interaction between WKS1.1 and tAPX.

(A) CoIP of WKS1.1 and tAPX1 in Bobwhite control (no-WKS1) and transgenic plants overexpressing TAP-WKS1.1 fusion protein. The arrow indicates the position of the mature tAPX1 protein detected by anti-tAPX rabbit antibody. 1 and 2 indicate samples from different transgenic events and from two different control plants (biological repeats).

(B) Loading control. Total protein from TAP-WKS1.1 transgenic plants and Bobwhite control analyzed with anti-tAPX rabbit antibody. All CoIP assays were performed with equal amounts of total protein (measured with a BCA protein quantification kit; Yeasen).

The Bobwhite transgenic plants transformed with the WKS1.1-GFP construct were all susceptible to *Pst* (Supplemental Figure 7A). This result differed from the partial resistance to *Pst* observed in the wheat plants transformed with NP:WKS1.1 (Figures 1F and 1G ; Fu et al., 2009) or Ubi:TAP-WKS1.1 (Supplemental Figure 7B). To explore the possible causes for these differences, we tested the effect of GFP and TAP tags at the N and C terminus of WKS1.1. The addition of GFP or TAP tags at the C terminus of WKS1.1 blocked its ability to form homodimers and to interact with tAPX in Y2H assays (Supplemental Figure 7B). When the tags were placed in the N terminus of WKS1, we obtained different results in the Y2H assays. TAP-WKS1.1 showed homodimers and a strong interaction with the full-length tAPX, but GFP-WKS1.1 showed weak homodimer formation and no interaction with tAPX. These results suggest that a disruption of the C-terminal region of WKS1.1 does not affect its subcellular localization but can have a negative impact on WKS1 protein interactions and its ability to confer resistance to *Pst*.

To provide further support for WKS1.1 localization to chloroplasts, we performed in vitro import assays using chloroplasts isolated from pea (*Pisum sativum*) seedlings and radiolabeled WKS1.1 protein with or without a GFP tag. When the nontagged WKS1.1 was examined by the assay, three major bands of 72, 66, and <50 kD were recovered in the integral membrane fraction, which was obtained by centrifugation after lysis with an alkaline buffer (Figure 6A, lane 4). Among the recovered proteins, the 72-kD band appears to correspond to the full-length WKS1.1 translation product (Figure 6A, lane 1). A chloroplast-import time-course assay showed the increase of the 66-kD band from 3% of the total WKS1.1 protein after 5 min to 25% after 40 min (Figure 6B, compare lanes 2 and 5). These results suggest that the 66-kD band was derived from the 72-kD protein during the assay; thus, we named it as mature-WKS1.1 (M-WKS1.1). Postimport treatment of chloroplasts with thermolysin, a protease that has access to surface-exposed proteins (Cline et al., 1984), resulted in degradation of the 72-kD band but M-WKS1.1 remained intact (Figure 6A, lane 6). The activity of the protease in the assay was confirmed by treating an aliquot of the same sample in the presence of detergent (Figure 6A, lane 7). Additional controls included assays without detergent using an outer membrane protein DGD1 (Froehlich et al., 2001), which was digested (Supplemental Figure 8, lane 4), and an inner membrane protein Tic40 (Stahl et al., 1999), which was resistant (Supplemental Figure 8, lane 9). Figure 6C shows that the larger fusion protein WKS1.1-GFP is also imported into the chloroplast. As in the nontagged WKS1.1, the imported protein (resistant to thermolysin) migrated slightly faster (~6 kD) than the precursor protein used for the assay. These data suggest that the ~6-kD truncation occurs in the N terminus of WKS1.1. The START domain alone was also recovered in the chloroplast

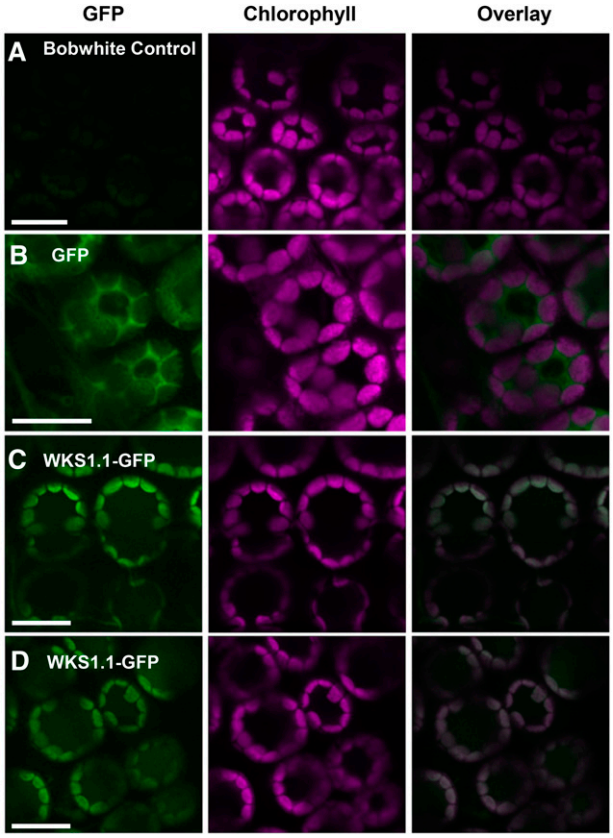

Figure 5. WKS1.1 Is a Chloroplast Protein in Wheat.

(A) Background fluorescence of nontransgenic Bobwhite control. Bar = 10 μm.
(B) Green fluorescence of free GFP in transgenic Bobwhite is observed in the cytosol (surrounding the chloroplasts and the central vacuole). Bar = 10 μm.
(C) and **(D)** Green fluorescence of WKS1.1-GFP fusion in transgenic wheat lines AB53-81a-2-4 and AB-53-62a-1-2 colocalizes with chlorophyll autofluorescence in chloroplasts. Bar = 10 μm.

integral membrane fraction (Figure 6D, lane 4) but was degraded by thermolysin (Figure 6D, lane 6). Taken together, these results confirm the chloroplast localization of WKS1.1. They also show that the START domain may play a role in WKS1.1 targeting of the chloroplast but that it is not sufficient to be imported into the chloroplast when separated from the N terminus of WKS1.1.

WKS1.1-Kinase Phosphorylates tAPX Protein in Vitro and in Planta

To test if WKS1 phosphorylates tAPX, we first purified the kinase portion of WKS1 (KA) and the full-length tAPX using a 6X His tag. We then incubated tAPX with KA and ATP, and samples lacking tAPX or ATP as negative controls. We then stained the extracted proteins with a fluorescent dye that specifically binds to phosphorylated peptides. The fluorescence bound to the protein was significantly higher in the samples with ATP than in the samples without ATP ($P < 0.0001$; Figure 7A), confirming the presence of phosphorylated peptides. In the presence of ATP, the samples with both KA and tAPX showed significantly higher fluorescence than the sample with KA alone ($P < 0.05$; Figure 7A), suggesting tAPX phosphorylation. However, high levels of fluorescence were also detected in the sample containing KA without tAPX, indicating that the WKS1-kinase is capable of autophosphorylation.

To confirm the WKS1-kinase phosphorylation of tAPX, we used two different in vitro assays. First, we performed the kinase reaction with radioactive [γ-^{32}P]ATP, WKS1-kinase, and tAPX and separated the products by SDS-PAGE. As a control, we used a similar sample replacing tAPX by PPIP5K1-like, which is not phosphorylated by WKS1-kinase. Both samples showed a strong signal for a small band corresponding to the autophosphorylated WKS1-kinase (Figure 7B, arrowhead), but only the sample with the tAPX protein showed an additional phosphorylated product of the size expected for tAPX (Figure 7B, lane 2, arrow). We then used a Phos-tag SDS-PAGE retardation assay. The tAPX protein from the samples with the WKS1-kinase and ATP showed retardation relative to the samples without ATP (Figure 7C). Taken together, these experiments indicate that the WKS1-kinase is able to phosphorylate tAPX in vitro.

To test the ability of WKS1 to phosphorylate tAPX in planta, we first extracted intact chloroplasts from nontransgenic wheat variety Bobwhite (control without *WKS1*) and from three independent transgenic Bobwhite plants previously transformed with a genomic copy of *WKS1* (Fu et al., 2009). In a Phos-tag SDS-PAGE retardation assay using the tAPX antibody, we observed that the tAPX proteins extracted from intact chloroplasts from the three independent Bobwhite-WKS1 transgenic plants were retarded compared with the sample from the nontransgenic Bobwhite control (Figure 7D). This result supports the hypothesis that WKS1 is targeted to the wheat chloroplast and phosphorylates tAPX in planta.

WKS1.1 Reduces tAPX Activity in Vitro and in Planta

To address the consequence of tAPX phosphorylation, we first investigated the biochemical characteristics of the *T. monococcum* tAPX protein. The activity of the recombinant tAPX protein prepared from *Escherichia coli* was significantly increased ($P < 0.001$) in the presence of 5 mM $MgCl_2$ and greatly reduced ($P < 0.001$) in the presence of $CaCl_2$ and $FeCl_3$ compared with a buffer with no additional ions (Supplemental Figure 9A). The tAPX protein had peroxidase activity in a wide range of pHs (5.0 to 8.0) with an optimum at 6.0 (Supplemental Figure 9B). Further tAPX activity experiments used pH 6.0 and a 5 mM $MgCl_2$ concentration.

An equal amount of tAPX recombinant protein was mixed for 3 h with WKS1.1-kinase/ATP, GST/ATP (negative control), or WKS1.1-kinase without ATP, and the activity of tAPX was quantified. tAPX samples mixed with GST/ATP or with WKS1.1 protein without ATP had similar tAPX-specific activity (1.54 versus 1.57 nmol ascorbic acid min^{-1} μg $protein^{-1}$, *t* test, $P = 0.91$), indicating that the physical binding of WKS1 with tAPX has little effect on tAPX activity (Figure 8A). However, in the samples including both WKS1.1 protein and ATP, tAPX activity was reduced by roughly 40% ($P < 0.05$; Figure 8A). This result indicates that the phosphorylation by WKS1.1 reduces tAPX activity in vitro.

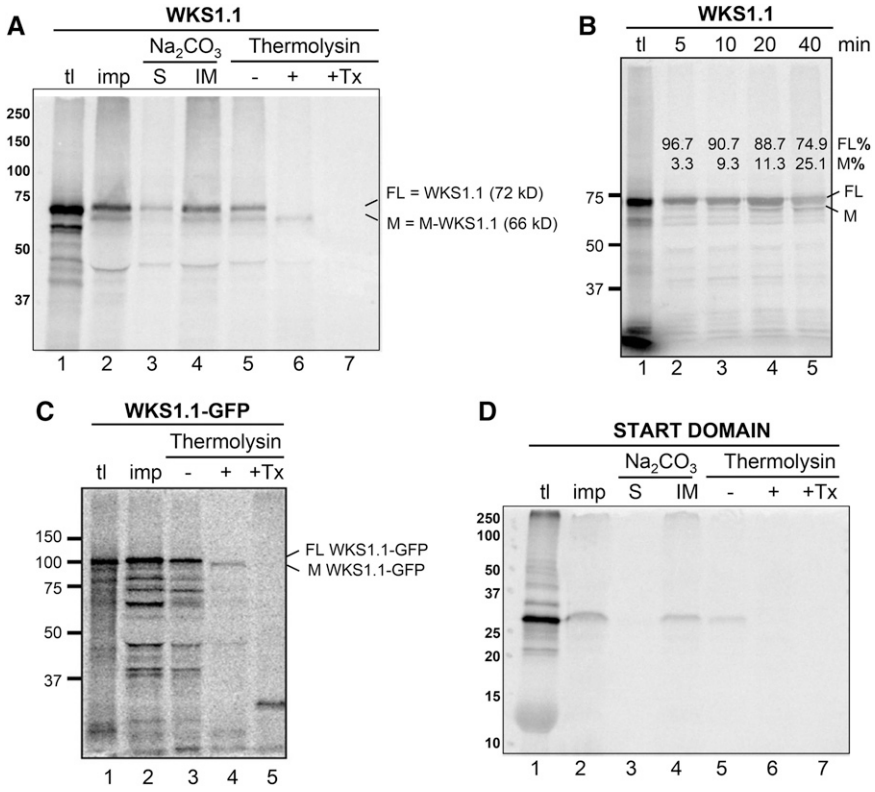

Figure 6. WKS1.1 Chloroplasts Import Assays.

(A) Radiolabeled full-length WKS1.1 protein incubated with intact chloroplasts. tl = 10% of translation products used for the import assay; imp. = proteins in intact chloroplasts recovered after a 20-min import reaction; Na_2CO_3 = chloroplasts lysed with 0.1 M Na_2CO_3 and fractionated by centrifugation into a supernatant that contained soluble proteins (S) and a pellet that contained integral membrane proteins (IM); thermolysin = chloroplasts incubated on ice for 30 min without (−) or with (+) thermolysin, or with thermolysin and 2% (v/v) Triton X-100 (Tx). Radiolabeled proteins were visualized using a phosphor imager: FL; full-length WKS1.1 (72 kD); M, processed M-WKS1.1 (66 kD).

(B) Radiolabeled full-length WKS1.1 protein incubated with intact chloroplasts for the time indicated at the top of the gel and analyzed as described in the legend of **(A)**. Intensity of each band relative to the total WKS1.1 protein (FL+M) is indicated above the bands.

(C) and **(D)** Radiolabeled WKS1.1-GFP fusion protein **(C)** and radiolabeled START domain protein **(D)** incubated with intact chloroplasts and analyzed as described in the legend of **(A)**.

The sizes of molecular mass markers in kilodaltons are shown to the left of each image. Import of control proteins DGD1 (located at the outer membrane) and Tic40 (located at the inner membrane) can be found in Supplemental Figure 8.

To confirm these results in planta, we measured APX activity in soluble and thylakoid fractions extracted from leaves of Bobwhite plants transformed with either NP:GFP (control) or NP:WKS1 (independent transgenic lines 26b-15, 26b-6, and 17a-15; Fu et al., 2009). The three NP:WKS1 transgenic plants showed significantly lower APX activity than the control in the thylakoid fraction (31 to 49% reduction, $P < 0.05$ one event and $P < 0.01$ two events; Figure 8B). No significant difference in APX activity was detected between genotypes in the soluble fraction (Figure 8C), suggesting that the reduced APX activity is specific to the thylakoid-associated tAPX.

To test if a reduction in tAPX activity independent of WKS1 can contribute to *Pst* resistance, we used a wheat line carrying a deletion of the B-genome copy of *tAPX*, henceforth referred to as Δ*tAPX-6B* (Danna et al., 2003). This mutation was previously associated with a reduction in total tAPX activity and with reduced photosynthetic activity and biomass accumulation under high light intensity (Danna et al., 2003). We crossed this mutant with the Ubi:TAP-WKS1.1 transgenic Bobwhite, self-pollinated the F1 hybrid, and generated an F2 population segregating for Ubi:TAP-WKS1.1 and Δ*tAPX-6B.* Plants carrying the WKS1.1 transgene showed partial resistance to *Pst*, whereas those without this transgene were susceptible (Figure 8D). The presence or absence of the Δ*tAPX-6B* mutation did not alter significantly the reaction to *Pst* in the plants with (partial resistance) and without WKS1.1 (susceptible; Figure 8D). This result suggests that the reduction of tAPX activity conferred by the Δ*tAPX-6B* mutation in this experiment was not sufficient to enhance resistance to *Pst*.

Transgenic Wheat Lines with Multiple WKS1 Copies Show Accelerated Leaf Senescence

In the original study of *WKS1* (Fu et al., 2009), we noticed that some of the *Pst*-resistant transgenic wheat plants that contained

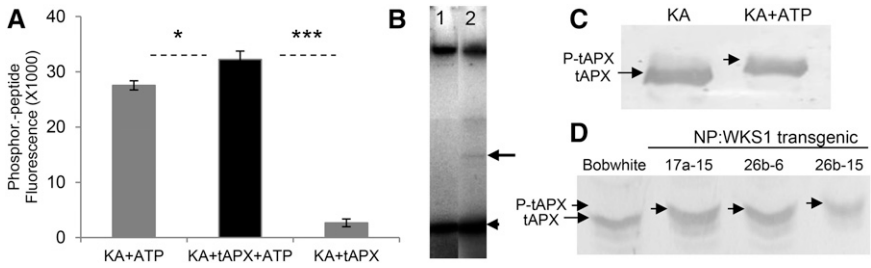

Figure 7. WKS1-Kinase Phosphorylates tAPX Protein in Vitro and in Vivo.

(A) Phosphofluorescence generated by autophosphorylation of the WKS1-kinase domain (KA+ATP) and by additional phosphorylation of tAPX by KA (KA+tAPX+ATP). The KA+tAPX control contained no ATP. Data represent the mean of five replications, and error bars are standard errors of the means. *$P < 0.05$ and ***$P < 0.001$.

(B) Phosphoimage of PPIP5K-like (lane 1, control) and tAPX (lane 2), both incubated with WKS1-kinase domain (KA) and [γ-^{32}P]ATP. The arrow indicates the phosphorylated tAPX and the arrowhead the autophosphorylated KA. PPIP5K protein is not phosphorylated by KA.

(C) Gel retardation of tAPX protein after WKS1-kinase phosphorylation initiated by ATP addition. tAPX was detected by anti-APX antibody. tAPX and P-tAPX indicate the position of tAPX protein before and after phosphorylation, respectively.

(D) Immunoblot of Phos-tag SDS-PAGE of proteins extracted from chloroplasts of nontransformed Bobwhite and three different transformants containing NP:WKS1 (17a-15, 26b-6, and 26b-15). Proteins were detected with anti-APX antibody.

multiple copies of the *WKS1* genomic region showed earlier senescence of the lower leaves than the nontransgenic control in the absence of the pathogen. To validate this preliminary observation, we selected two independent transgenic events (17a and 26b) with multiple WKS1 copies and compared two plants of each event with the nontransgenic control. Eight plants from each genotype were grown in a controlled environment chamber under long-day photoperiod (16 h light/8 h dark), and the second leaf of each plant was compared at the same developmental stage. All four transgenic plants showed accelerated senescence compared with the nontransgenic control (Figure 9A).

To quantify these differences in senescence, we measured relative chlorophyll content using a hand-held chlorophyll meter (SPAD-502; Minolta) in the midsection of the different leaves of eight transgenic and eight control plants at the time of ear emergence (10 measurements per individual leaf). Significant reductions in relative chlorophyll content in the three older leaves (Figure 9B, 1st to 3rd leaf, Dunnett's test, $P < 0.01$) were detected in the four transgenic genotypes relative to the nontransgenic Bobwhite control. These results confirmed that the presence of multiple copies of *WKS1* in the Bobwhite plants transformed by bombardment (Fu et al., 2009) is associated with early leaf senescence. Using the Amplex red hydrogen peroxide/peroxidase assay kit (Molecular Probes), we confirmed that the transgenic *WKS1* plants had significantly higher levels of H_2O_2 than the wild-type control (statistical contrast between the wild type and four transgenic lines, $P = 0.011$; Figure 9C).

DISCUSSION

WKS1 Is Targeted to the Chloroplast

The localization of WKS1.1 to the chloroplast was an unexpected result because there are only a few examples of resistance proteins targeted to this organelle, including Arabidopsis RESISTANCE TO PHYTOPHTHORA1 (Belhaj et al., 2009) and the chloroplastic/cytoplasmic protein NRIP1, which in association with the NB-LRR immune receptor "N" is responsible for *Tobacco mosaic virus* recognition and resistance in *Nicotiana* (Caplan et al., 2008). This chloroplast localization was also unexpected because no chloroplast transit peptide (Shi and Theg, 2013) was predicted for WKS1. However, proteomic studies have shown that ~10% of the chloroplast proteins lack a cleavable transit peptide (Armbruster et al., 2009). Some of these proteins use an alternative chloroplast targeting pathway that involves the endoplasmic reticulum (ER) and the Golgi apparatus (Radhamony and Theg, 2006). However, this pathway may not be relevant for WKS1, which lacks an ER signal peptide and can be imported into purified chloroplasts in vitro.

WKS1 interacts with VAP1-3 (Supplemental Figure 4), which belongs to a class of proteins previously shown to be located in the ER and to be involved in membrane traffic (Loewen and Levine, 2005). We confirmed the interaction between WKS1.1 and VAP1-3 by bimolecular fluorescence in *N. benthamiana* protoplasts (Supplemental Figure 10) and initiated a screen for mutations in wheat VAP1-3 to test if this protein is required for the transport of WKS1.1 to the chloroplast.

Alternative Splice Variants *WKS1.1* and *WKS1.2* Exhibit Altered Properties and Function

WKS1 is present in several alternative splice variants, including the complete protein (WKS1.1), the major variant WKS1.2 that lacks the last exon, and several less frequent shorter variants (Fu et al., 2009). Alternative splicing is a widespread mechanism in animals and plants that increases diversity of transcripts (e.g., different RNA stability) and proteins (e.g., different subcellular localization, stability, or function) (Syed et al., 2012; Staiger and Brown, 2013). This seems to be also the case for WKS1 alternative splice variants, which differ in their abilities to form homodimers, to interact with other proteins, and to confer resistance to *Pst*. WKS1.2 and the shorter alternative splice variants all lack

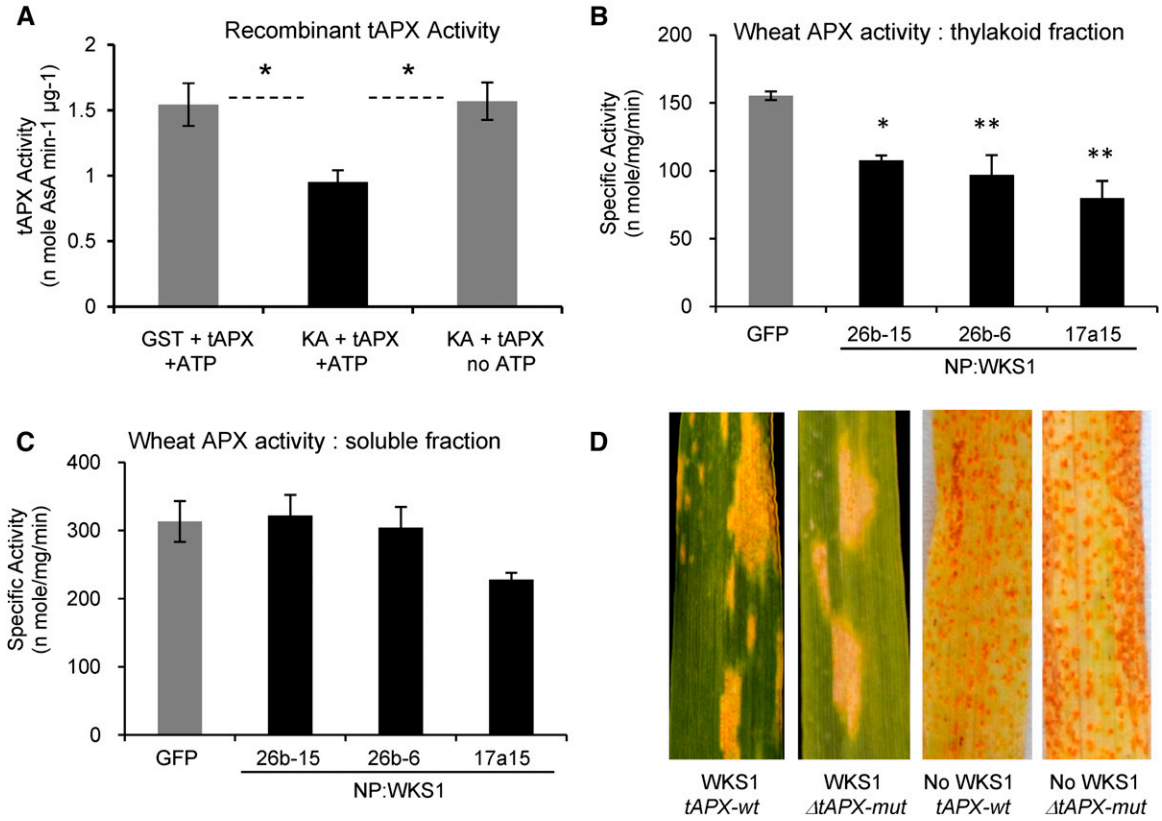

Figure 8. Effect of WKS1.1 on tAPX Activity in Vitro and in Planta.

(A) tAPX-specific activity in the presence of GST+ATP (negative control), KA+ATP, and KA without ATP ($n = 4$, *$P < 0.05$; KA = kinase alone). Error bars are standard errors of the means.

(B) APX-specific activity in thylakoid fractions from Bobwhite plants transformed with NP:GFP (control) and with NP:WKS1 (genomic). Dunnett's tests, *$P < 0.05$ and **$P < 0.01$

(C) APX-specific activity in soluble fractions extracted from the same genotypes as in **(B)**. No significant differences were detected.

(B) and **(C)** 26b15, 26b6, and 17a15 are three independent transformation events with a genomic copy of *WKS1* (Fu et al., 2009). Error bars are standard errors of the means.

(D) F3 families segregating for Δ*tAPX-6B* deletion and Ubi:TAP-WKS1.1 transgene infected with *Pst* race PST130. Plants carrying WKS1.1 showed partial resistance and plants without the transgene were susceptible. The Δ*tAPX-6B* deletion did not affect *Pst* resistance.

the last 11 amino acids of the START domain, which include several amino acids that are conserved across plants and mosses (Fu et al., 2009). The addition of a GFP tag to the C terminus of WKS1.1 limited the formation of homodimers, the interaction with tAPX, and the resistance to *Pst*, confirming the importance of this region in WKS1.1 function. Since WKS1.1-GFP is imported into the chloroplasts as efficiently as the full-length WKS1.1 (Figure 6C), the *Pst* susceptibility of the wheat plants transformed with WKS1.1-GFP (Supplemental Figure 7A) is most likely due to the inability of WKS1.1-GFP to form homodimers and to interact with tAPX or other proteins (Supplemental Figure 7B).

The C-terminal region of the START domain is also critical for normal function of several human START proteins (Alpy and Tomasetto, 2014). This region includes an α-helix that can interact with lipid membranes and regulate the accessibility of the lipid ligand to the lipid binding pocket (Alpy and Tomasetto, 2014). The truncation of the C-terminal region of the START domain in WKS1.2 may alter similar functions in wheat, resulting in nonfunctional proteins. Since only WKS1.1 is effective against *Pst*, the increase in *WKS1.1* transcript levels relative to *WKS1.2* during the first 3 d of *Pst* infection (Fu et al., 2009) might have an impact on the resistance response.

WKS1 START Domain Has Lipid Binding Ability

The mammalian START proteins bind diverse ligands, such as cholesterol, oxysterols, phospholipids, sphingolipids, and possibly fatty acids (Clark, 2012), and several of these ligands appear to be shared by plant START domains (Schrick et al., 2014). However, lipid ligands for plant START domains have been studied only for Arabidopsis homeodomain leucine zipper (HD-Zip) transcription factors (Schrick et al., 2014). These START domains are distantly related to the START domain present in Arabidopsis EDR2 (Schrick et al., 2004), which is the

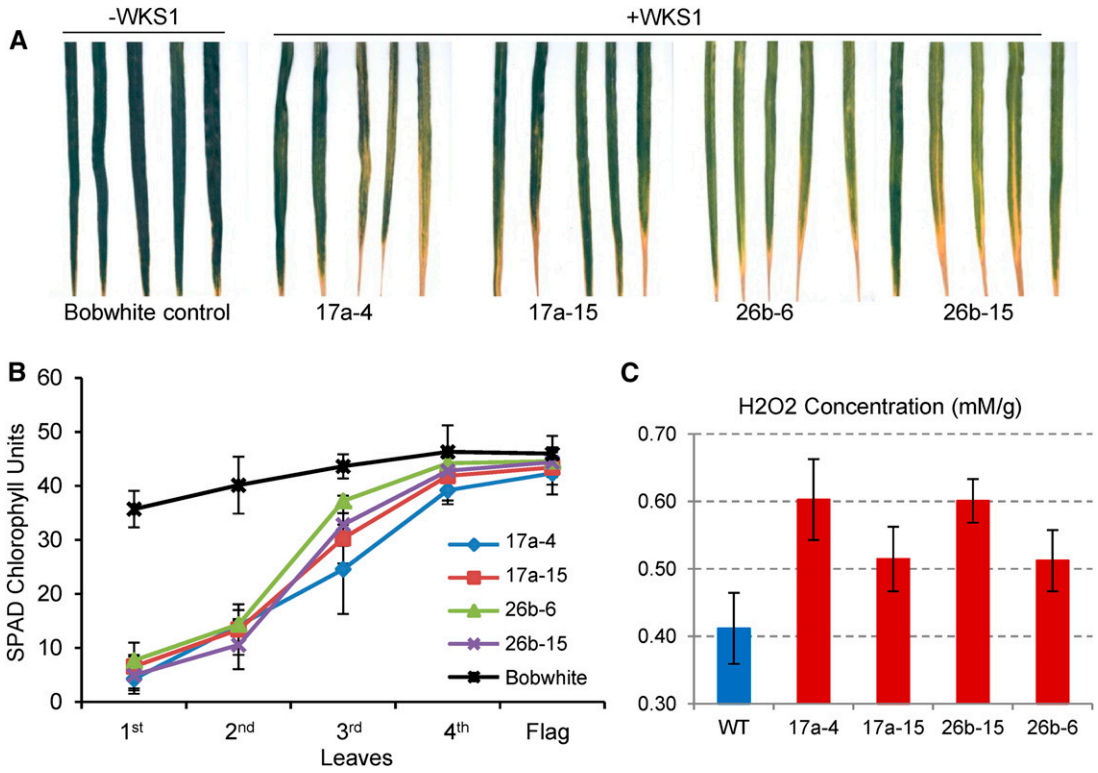

Figure 9. Leaf Necrosis in Transgenic Wheat with Multiple Genomic Copies of *WKS1*.

(A) Early senescence of 2nd leaves of *WKS1* transgenic plants from two independent events (sibs 17a-4 /17a-15 and sibs 26b-6/26b-15) in the absence of *Pst*. Nontransgenic Bobwhite serves as control.

(B) Relative SPAD chlorophyll units of *WKS1* transgenic or Bobwhite control plants. Samples were collected from the midsection of each leaf from the oldest (1st) to the youngest (flag leaf). Data points are means of eight measurements per leaves from 10 individual plants. Error bars are standard errors of the means.

(C) Quantification of H_2O_2 using an Amplex red hydrogen peroxide/peroxidase assay kit (Molecular Probes). Transgenic plants showed significantly higher H_2O_2 levels than the wild-type control (statistical contrast between the wild type and four *WKS1* transgenic lines, P = 0.011). Samples were collected from the mid-region of the second oldest leaf from five to nine 5-week-old plants per genotype (growth conditions: 16 h light at 25°C and 8 h dark at 20°C). Error bars are standard errors of the means.

closest to the WKS1 START domain (Fu et al., 2009). The START domain of EDR2 is more closely related to the human STARD14/D15 subfamily than to the plant START domains in the HD-Zip transcription factors (Schrick et al., 2004), which suggests that this START domain group likely originated before the divergence of plants and animals. Similarly to WKS1, STARD14 active form is a dimer and presents alternative splicing forms with distinct START domain C-terminal ends (Alpy and Tomasetto, 2014).

The lipid blots analyzed here showed that the START domain from WKS1 has affinity for PA and several PIPs (Figure 2A). START domains of Arabidopsis HD-Zip transcription factors PDF2 and GL2 also show affinity for PA, among various other phospholipids, but affinity for PIPs has not been described to our knowledge for other plant or animal START domains (Alpy and Tomasetto, 2014; Schrick et al., 2014). We currently do not know if this is because WKS1.1 START domain has a unique lipid affinity or because PIPs have not been extensively tested in START domain binding assays (Schrick et al., 2014). Both PA and PIPs are important molecules in cellular signaling and trafficking (Munnik and Vermeer, 2010; Testerink and Munnik, 2011) and have been implicated in plant disease resistance (de Jong et al., 2004; Park et al., 2004; Andersson et al., 2006; Raho et al., 2011; Hung et al., 2014). It would be interesting to investigate if there is a connection between the ability of WKS1 to bind PA and PIPs and its ability to detect the presence of *Pst*.

WKS1 Phosphorylation of tAPX Is Associated with H_2O_2 Accumulation and Cell Death in *Pst*-Infected Regions

In the absence of the pathogen, the wild-type allele of WKS1 seems to have a limited negative effect on yield performance of hexaploid wheat, since near-isogenic lines differing in the presence of *WKS1* and the tightly linked *GPC-B1* gene showed no significant yield differences in multiple environments (Brevis et al., 2008). However, compared with the nontransgenic control, transgenic wheat plants transformed by bombardment and including multiple genomic copies of *WKS1* (Fu et al., 2009) showed premature senescence of the older leaves (Figures 9A and 9B),

which was associated with significantly higher levels of H_2O_2 (Figure 9C). Rapid increases in ROS levels play an important role in disease resistance by triggering cell death near infection sites and thereby limiting pathogen proliferation (Bradley et al., 1992; Levine et al., 1994; Greenberg, 1996).

tAPX plays a central role in the detoxification of H_2O_2 generated during photosynthesis. Using the reducing power of ascorbate and other endogenous antioxidants, tAPX catalyzes the reduction of H_2O_2 to water (Caverzan et al., 2012). Arabidopsis tAPX knockout mutants show significantly higher levels of H_2O_2 than the wild type after exposure to intense light (Maruta et al., 2010). Similarly, hexaploid wheat plants lacking the *tAPX-6B* homoeolog show reduced photosynthesis and increased susceptibility to rapid oxidative stress (Danna et al., 2003). Based on the previous observations, we hypothesize that the reduced tAPX activity in planta observed in the presence of WKS1.1 contributes to the accumulation of H_2O_2 and the initiation of the progressive cell death response characteristic of the WKS1.1 partial resistance reaction to *Pst* (Figure 1).

Since programmed cell death, developmental senescence, and responses to pathogens are linked through complex genetic regulatory networks (Pavet et al., 2005; Feng et al., 2014), we also evaluated the effect of the Δ*tAPX-6B* mutation on the modulation of the *WKS1.1* responses to *Pst*. The deletion of one of the three tAPX homoeologs in hexaploid wheat (Δ*tAPX-6B*) was not sufficient to confer resistance to *Pst* in the absence of WKS1.1. This result suggests that the WKS1 mechanism to detect *Pst* is more complex than a simple reduction in the threshold of ROS-induced senescence and may involve the detection of changes in PA or PIP signaling through the START domain or interactions with other pathogen or wheat proteins. Among the plants carrying *WKS1.1*, the presence of the Δ*tAPX-6B* mutation was not associated with obvious differences in the levels of resistance (Figure 8D). However, it is important to consider that these observations were made in an F2:3 population that was still segregating for flowering time and other traits. The detection of subtle differences in *Pst* resistance or H_2O_2 accumulation associated with the Δ*tAPX-6B* mutation will require further experiments in a uniform genetic background.

A Working Model for WKS1 Partial Resistance Mechanism

Figure 10 summarizes our current working model for the role of WKS1 in the induction of cell death. Previous results have shown that *Pst* infection triggers an increase in *WKS1.1* and a decrease in *WKS1.2* transcripts levels (Fu et al., 2009). According to this working model, the increased levels of the functional WKS1.1 variant result in increased phosphorylation of tAPX, reduced tAPX activity, and reduced ability of the cells to detoxify ROS. The gradual accumulation of ROS ultimately results in cell death and partial resistance to *Pst*. The WKS1-mediated resistance process takes approximately 1 week to contain the progression of the *Pst* infection (Supplemental Figure 1). This is several days longer than previously described hypersensitive responses to *Pst* triggered by *R* genes, which result in necrotic cells within 2 to 4 dpi (Wang et al., 2007). The slower resistance response associated with WKS1 allows some *Pst* intercellular growth and sporulation and results in a partial resistance response (Figure 1; Supplemental Figure 1).

Although the role of the START domain in this mechanism is still not clear, we know that this domain is required for *Pst* resistance, since a single amino acid mutation in the hydrophobic pocket of the START domain in the *wks1e* mutant (Fu et al., 2009) or the addition of a GFP tag at the C-terminal end of the START domain (Supplemental Figure 7A) results in complete susceptibility. One possible role of the START domain is to modulate WKS1 ability to form homodimers and to interact with tAPX and other downstream proteins. Ligand binding by the START domain has been also proposed as a mechanism to regulate the activities of adjacent domains, such as Rho-GAP and thioesterase domains in the human START domain-containing protein STARD14 (Schrick et al., 2014). Results from Figure 3D are consistent with this hypothesis: The kinase domain without the START domain is able to form homodimers in the stringent Y2H assays (SD -L-W-H-A), but the complete WKS1.1 protein domain can form homodimers only under low stringency Y2H assays (SD -L-W-H; Figure 3D). These results suggest that, under certain physiological conditions, the presence of the START domain can reduce the strength of the protein-protein interactions mediated by the kinase and the interdomain.

The particular *Pst* resistance mechanism described here for WKS1.1 may have implications in the utilization of this gene in agriculture. The combination of resistance genes with different modes of action against the same pathogen has been proposed as a strategy to extend the durability of deployed resistance genes (Lowe et al., 2011). In this context, WKS1.1 is an interesting candidate for deployment in gene pyramids with other *Pst* resistance genes. Only the test of time will determine if this strategy will result in more stable resistance against this devastating pathogen.

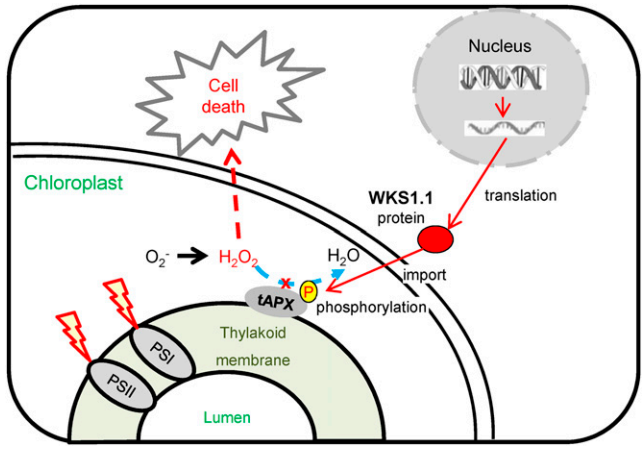

Figure 10. Working Model of WKS1.1 Regulation of Cell Death.

The WKS1.1 protein is imported into the chloroplast, where it phosphorylates tAPX, reducing its ability to detoxify the H_2O_2 generated by photosynthesis. The dotted blue line indicates reduced peroxidase activity, and the dotted red line indicates increased H_2O_2 concentration, which causes cell death. PSI, photosystem I; PSII, photosystem II.

METHODS

Plant Materials

Hexaploid wheat (*Triticum aestivum*) breeding line UC1041 and a near isogenic line with the *WKS1* gene, together with two previously described homozygous *WKS1*-kinase mutants wks1b and wks1d (susceptible) and their respective wild-type sister controls (resistant) (Fu et al., 2009), were used for the *Pst* infection time course. Methods used for the evaluation of the different stages of *Pst* infection are described in detail in Supplemental Methods 1. All the chamber experiments were conducted under a long-day photoperiod (16 h light/8 h dark). For the stripe rust inoculations, plants were placed in a dew chamber without light at 10°C for 24 h. Plants were inoculated, transferred to 25°C, and then evaluated for resistance (3, 6, 10, and 13 dpi for the time-course experiment).

The hexaploid wheat varieties 'Glasgow' and 'Bobwhite' were used for the transformation experiments. The specific genes, promoters, vectors, and selection methods used for each variety are summarized in Table 1, in the transgenic method section below, and in Supplemental Methods 2.

A deletion mutant of the B-genome copy of *tAPX* in the hexaploid wheat variety 'Sinvalocho MA,' kindly provided by R.A. Ugalde from the Instituto Nacional de Tecnología Industrial, Argentina (Sacco et al., 1998), was crossed with a transgenic Bobwhite overexpressing *WKS1* (Ubi:TAP-WKS1) to study the effect of WKS1 on tAPX in planta. The hybrid was self-pollinated, and sister lines homozygous for the *tAPX-6B* deletion, the *WKS1.1* transgene, or for both were selected from the segregating F2 plants using primers UbiP-F1 and TAP-R254 for Ubi:TAP-WKS1.1, and TAPX-6B-F and TaAPX-6B-R for the *tAPX-6B* deletion (Supplemental Table 2). Plants were inoculated with *Pst* race PST130 at 10°C and then transferred to 25°C and evaluated for resistance 3 weeks later.

Wheat Transformation

To characterize the effect of *WKS1* on leaf senescence, we used transgenic plants that carry a complete genomic copy of *WKS1* including 3.5-kb region upstream from the start codon and 1.4 kb downstream from the stop codon (Fu et al., 2009). We selected plants from two transformation events (17a and 26b) that had the highest transcript levels of WKS1 (Fu et al., 2009). These transgenic lines were developed by bombardment and have different *WKS1* copy numbers (Fu et al., 2009).

In addition, we developed transgenic wheat lines for five new constructs specifically for this study (Table 1). To determine the effect of WKS1 alternative splice variants on *Pst* resistance, we generated transgenic Glasgow plants including either the *WKS1.1* or the *WKS1.2* coding regions under the control of the 3.5-kb native promoter (NP:WKS1.1 and NP:WKS1.2). These transgenic lines were developed at the National Institute of Agricultural Botany using the Seed Inoculation Method licensed from Biogemma (Risacher et al., 2009).

Transgenic Bobwhite lines Ubi:TAP-WKS1.1 and NP:WKS1.1-GFP (Table 1) were developed by bombardment using methods described before (Okubara et al., 2002) and summarized briefly in Supplemental Methods 2. The Ubi:TAP-WKS1.1 transgenic wheat plants expressing a fusion protein between the TAP tag (Rohila et al., 2006) and WKS1 under the regulation of the maize (*Zea mays*) *Ubiquitin* promoter were used for CoIP experiments and to study the effect of the overexpression of *WKS1.1* in the presence and absence of the *tAPX-6B* mutation. The NP:WKS1.1-GFP transgenic wheat plants expressing a fusion protein between WKS1.1 and GFP under the regulation of the *WKS1* promoter region (3.5 kb) was used to study the subcellular localization of WKS1.1 in vivo. As a control, we developed additional transgenic wheat plants expressing GFP under the regulation of the same promoter region (NP:GFP). Transgenic lines were evaluated for resistance to race PST-08/21 (Cantu et al., 2013) and PST130 (Cantu et al., 2011).

In Vitro Lipid Assays

To test the ability of the full-length WKS1.1 and WSK1.2 and of their respective START domains to bind lipids, we generated four GST fusions and expressed them in wheat germ extracts as described in Supplemental Methods 3. We then tested the ability of these four GST-tagged proteins to bind lipid using two different lipid strips developed by Echelon Biosciences. The first one included 100 pmol of 15 different membrane lipids and the second one included decreasing concentrations of mono-, di-, and triphosphate PIPs (Figure 2). Methods for incubation, washing, and detection are described in Supplemental Methods 3.

Y2H Assays and Library Screening

Pairwise Y2H interactions were performed using the Matchmaker Gold yeast two-hybrid system (Clontech Laboratories) as described before (Li et al., 2011). Gateway-compatible versions of the pGBKT7 (bait) and pGADT7 (prey) vectors were provided by Richard Michelmore (University of California, Davis) and were designated pLAW10 and pLAW11, respectively. Primers used to generate the different yeast constructs are listed in Supplemental Table 2, and the Y2H methods and controls are described in Supplemental Methods 4. To find WKS1 interactors, we screened a cDNA library generated from RNA extracted from leaves of tetraploid wheat infected with *Puccinia striiformis* race PST113 (Yang et al., 2013) as described in Supplemental Methods 5.

In Vitro Chloroplast Import Assays

Plasmids carrying coding sequences for the full-length WKS1.1 protein, the WKS1.1-GFP fusion, and the WKS1.1-START domain were prepared as described in Supplemental Methods 6. Plasmids for DGD1 and Tic40 were as described previously (Froehlich et al., 2001; Tripp et al., 2007). Procedures of chloroplast import assays were described before (Midorikawa and Inoue, 2013).

CoIP

To validate the interaction between WKS1 and tAPX observed in the Y2H experiments, we performed a CoIP experiment, as described in detail in Supplemental Methods 7. Briefly, a total protein extract of leaves from Ubi:TAP-WKS1.1 transgenic plants overexpressing WKS1.1 was mixed and incubated with IgG Sepharose beads. The TAP-tagged proteins were released by digestion with tobacco etch virus protease and incubated with calmodulin-agarose beads. The eluted proteins were precipitated and loaded onto a 4 to 15% gradient polyacrylamide gel for SDS-PAGE. Proteins were transferred to a nitrocellulose membrane and tAPX was detected by protein gel blot using a commercial rabbit anti-tAPX antibody (Agrisera; catalog number AS08 368).

Recombinant Protein Purification

The *WKS1.1* kinase domain from *Triticum turgidum* ssp *dicoccoides* and the full-length genes *tAPX* and *PPIP5K1*-like from *Triticum monococcum* accession DV92 were amplified by reverse transcription of leaf mRNA using primers described in Supplemental Table 2. The PCR products were ligated into vectors pET41b (*WKS1.1*-kinase), pET28a (*tAPX*), and pDEST17 (*PPIP5K1*-like), all of which have an N-terminal 6X His tag. Constructs were confirmed by sequencing and were transformed into BL21 (DE3) plysS-competent cells (Promega). Proteins were purified using the N-terminal 6X His tag with Ni-NTA resin (Pierce Biotechnology) as described in Supplemental Methods 8.

Phosphorylation Assays

To test the ability of the WKS1-kinase to phosphorylate tAPX, we mixed 2 μg of each recombinant protein in a kinase reaction buffer (100 mM PBS,

pH 7.5, 10 mM $MgCl_2$, 1 mM ascorbic acid, and 2 mM ATP) for 3 h at room temperature. Methods for the quantitative phosphofluorescence assay (Figure 6A), the in vitro phosphorylation assay separation in SDS-PAGE (Figure 6B), and the in vitro and in planta gel retardation assays (Figures 6C and 6D) are described in detail in Supplemental Methods 9. For the in planta gel retardation assays, we first isolated intact chloroplast from transgenic Bobwhite wheat plants transformed with NP:WKS1 and from nontransgenic Bobwhite lacking WKS1 as control. Proteins were extracted from the intact chloroplasts, and the tAPX protein was detected in protein gel blot using the same commercial rabbit anti-tAPX antibody described above. Controls for the in vitro assays included samples without ATP (Figure 6A) or with the PPIP5K1-like protein, which is not phosphorylated by the WKS1-kinase (Figure 6B).

Recombinant tAPX Activity Assays

tAPX Recombinant Protein

The tAPX recombinant protein was purified as described above and in Supplemental Methods 8. The activity of 2 μg of recombinant tAPX protein was first tested for its ability to decrease H_2O_2 concentration (Supplemental Methods 10). To analyze the effect of WKS1.1 phosphorylation on tAPX activity, we then mixed 2 μg of in vitro-translated WKS1.1 protein with 2 μg of tAPX recombinant protein in a kinase reaction buffer and incubated for 3 h at room temperature. tAPX activity was then determined as described in Supplemental Methods 10.

APX Protein Extracted from Wheat Plants

Wheat-soluble and thylakoid APX activity was compared between transgenic Bobwhite plants transformed with GFP (control) and NP:WKS1 (transgenic lines 26b-15, 26b-6, and 17a-15; Fu et al., 2009). Assays were performed following previously published protocols (Danna et al., 2003) described in detail in Supplemental Methods 10.

Accession Numbers

Sequence data from this article can be found in the GenBank/EMBL data libraries under accession numbers KJ614568 (tAPX), KJ614569 (VAP1), and KJ614570 (PPIP5K1-like).

Supplemental Data

Supplemental Figure 1. Pathogen Growth and Development in Interveinal Regions of Uvitex-Stained Leaves in Three Pairs of Hexaploid Wheat Isogenic Lines with and without *WKS1*.

Supplemental Figure 2. Wheat Plants Transformed with NP:WKS1.1 or NP:WKS1.2 and Inoculated with *Pst* Race PST-08/21.

Supplemental Figure 3. Effect of WKS1.1 Mutations on Homodimer Formation.

Supplemental Figure 4. Y2H Assays between WKS1 Variants and Interacting Proteins tAPX, VAP1-3, and PPIP5K1-Like.

Supplemental Figure 5. Western Blot Confirming that Mutant and Alternative Splice WKS1.2 Proteins Are Not Degraded in Negative Y2H Interactions in Figure 3 and Supplemental Figures 3 and 4.

Supplemental Figure 6. Interaction Between tAPX and Splice Variants WKS1.1 and WKS1.2 by Bimolecular Fluorescence Complementation.

Supplemental Figure 7. Effect of WKS1.1 Fusions with Tags at the N- or C-Terminal Regions on Interactions with Full-Length tAPX in Y2H Assays and on Resistance to *Pst*.

Supplemental Figure 8. Controls for the in Vitro Chloroplast Import Assays.

Supplemental Figure 9. Effect of Different Ions and pH on tAPX Activity in Vitro.

Supplemental Figure 10. Validation of the Interaction between VAP1-3 and WKS1.1 by Bimolecular Fluorescence Complementation in *N. benthamiana* Protoplasts.

Supplemental Table 1. Average Resistance of Plants Transformed with NP:WKS1.1 and NP:WKS1.2 and Inoculated with *Pst* Race PST-08/21.

Supplemental Table 2. Primers Used in This Study.

Supplemental Table 3. WKS1 Protein Interactors Detected in Y2H Screen and Their Y2H Interactions with Alternative Splice Variants WKS1.1 and WKS1.2 and Mutants (wks1a-e).

Supplemental Methods 1. Time Course of *Pst* Infection.

Supplemental Methods 2. Transgenic Lines.

Supplemental Methods 3. In Vitro Lipid Binding Assays.

Supplemental Methods 4. Yeast Two-Hybrid Assays.

Supplemental Methods 5. Wheat cDNA Y2H Library Screening and Validation.

Supplemental Methods 6. In Vitro Chloroplast Localization.

Supplemental Methods 7. Coimmunoprecipitation.

Supplemental Methods 8. Recombinant WKS1-Kinase, tAPX, and PPIP5K1-Like Protein Purification.

Supplemental Methods 9. Phosphorylation Assays.

Supplemental Methods 10. tAPX Activity Assays.

ACKNOWLEDGMENTS

This project was supported by National Research Initiative Competitive Grant 2011-68002-30029 (Triticeae-CAP) from the USDA National Institute of Food and Agriculture, by US-Israel BARD Grants US-4323-10C and IS-4628-13, by Division of Chemical Sciences, Geosciences, and Biosciences, Office of Basic Energy Sciences of the U.S. Department of Energy Grant DE-FG02-08ER15963, by the Major International Joint Research Project (31110103917) from the National Natural Science Foundation of China, and by the SCPRID Program (BB/J012017/1) from the Biotechnology and Biological Science Research Council. J.D. acknowledges the financial support of the Howard Hughes Medical Institute and Gordon & Betty Moore Foundation. J.-Y.G. is supported by The Program for Professor of Special Appointment (Eastern Scholar) at Shanghai Institutions of Higher Learning (SHH1322012) and the National Natural Science Foundation of China (31470386). C.U. and E.W. acknowledge financial support from the National Institute of Agricultural Botany Trust and thank M. Craze and S. Bowden for transformation of wheat variety Glasgow as well as R. LeFevre and R. Howells for technical assistance. A.D.-A. is supported by a Marie Curie fellowship. The USDA is an equal opportunity provider and employer. Mention of a specific product name by the USDA does not constitute an endorsement and does not imply a recommendation over other suitable products.

AUTHOR CONTRIBUTIONS

J.D., C.U., D.F., T.F., and J.-Y.G. designed the research. J.-Y.G. performed senescence and APX experiments and coordinated the

experiments. M.M. and L.E. performed the *Pst* time course. E.W., A.D.-A., and C.U. developed and characterized the NP:WKS1.1 and NP:WKS1.2 transgenic plants. A.B. developed the Ubi:TAP-WKS1.1 and NP:WKS1.1-GFP transgenic plants. D.C. characterized the cellular localization. X.W., K.W., K.L., and D.F. performed protein-protein interaction assays. H.L. and X.W. performed the bimolecular fluorescence complementation assays, and J.S. performed the lipid binding assays. T.M. conducted protein import assay using isolated chloroplasts, and T.M. and K.I. analyzed the data. J.-Y.G. wrote the first version of the article. All authors contributed to the analysis of the data and to the review of the article. J.D. revised the article, integrated the corrections, and produced the final version.

Received November 24, 2014; revised April 21, 2015; accepted April 26, 2015; published May 19, 2015.

REFERENCES

Alpy, F., and Tomasetto, C. (2014). START ships lipids across interorganelle space. Biochimie **96:** 85–95.

Andersson, M.X., Kourtchenko, O., Dangl, J.L., Mackey, D., and Ellerström, M. (2006). Phospholipase-dependent signalling during the AvrRpm1- and AvrRpt2-induced disease resistance responses in *Arabidopsis thaliana.* Plant J. **47:** 947–959.

Armbruster, U., Hertle, A., Makarenko, E., Zühlke, J., Pribil, M., Dietzmann, A., Schliebner, I., Aseeva, E., Fenino, E., Scharfenberg, M., Voigt, C., and Leister, D. (2009). Chloroplast proteins without cleavable transit peptides: rare exceptions or a major constituent of the chloroplast proteome? Mol. Plant **2:** 1325–1335.

Belhaj, K., Lin, B., and Mauch, F. (2009). The chloroplast protein RPH1 plays a role in the immune response of Arabidopsis to *Phytophthora brassicae.* Plant J. **58:** 287–298.

Bradley, D.J., Kjellbom, P., and Lamb, C.J. (1992). Elicitor- and wound-induced oxidative cross-linking of a proline-rich plant cell wall protein: a novel, rapid defense response. Cell **70:** 21–30.

Brevis, J.C., Chicaiza, O., Khan, I.A., Jackson, L., Morris, C.F., and Dubcovsky, J. (2008). Agronomic and quality evaluation of common wheat near-isogenic lines carrying the leaf rust resistance gene *Lr47.* Crop Sci. **48:** 1441–1451.

Cantu, D., Govindarajulu, M., Kozik, A., Wang, M., Chen, X., Kojima, K.K., Jurka, J., Michelmore, R.W., and Dubcovsky, J. (2011). Next generation sequencing provides rapid access to the genome of *Puccinia striiformis* f. sp. *tritici*, the causal agent of wheat stripe rust. PLoS ONE **6:** e24230.

Cantu, D., Segovia, V., MacLean, D., Bayles, R., Chen, X., Kamoun, S., Dubcovsky, J., Saunders, D.G.O., and Uauy, C. (2013). Genome analyses of the wheat yellow (stripe) rust pathogen *Puccinia striiformis* f. sp. *tritici* reveal polymorphic and haustorial expressed secreted proteins as candidate effectors. BMC Genomics **14:** 270.

Caplan, J.L., Mamillapalli, P., Burch-Smith, T.M., Czymmek, K., and Dinesh-Kumar, S.P. (2008). Chloroplastic protein NRIP1 mediates innate immune receptor recognition of a viral effector. Cell **132:** 449–462.

Caverzan, A., Passaia, G., Rosa, S.B., Ribeiro, C.W., Lazzarotto, F., and Margis-Pinheiro, M. (2012). Plant responses to stresses: Role of ascorbate peroxidase in the antioxidant protection. Genet. Mol. Biol. **35** (suppl.): 1011–1019.

Clark, B.J. (2012). The mammalian START domain protein family in lipid transport in health and disease. J. Endocrinol. **212:** 257–275.

Cline, K., Werner-Washburne, M., Andrews, J., and Keegstra, K. (1984). Thermolysin is a suitable protease for probing the surface of intact pea chloroplasts. Plant Physiol. **75:** 675–678.

Coll, N.S., Epple, P., and Dangl, J.L. (2011). Programmed cell death in the plant immune system. Cell Death Differ. **18:** 1247–1256.

Danna, C.H., Bartoli, C.G., Sacco, F., Ingala, L.R., Santa-María, G.E., Guiamet, J.J., and Ugalde, R.A. (2003). Thylakoid-bound ascorbate peroxidase mutant exhibits impaired electron transport and photosynthetic activity. Plant Physiol. **132:** 2116–2125.

de Jong, C.F., Laxalt, A.M., Bargmann, B.O.R., de Wit, P.J.G.M., Joosten, M.H.A.J., and Munnik, T. (2004). Phosphatidic acid accumulation is an early response in the Cf-4/Avr4 interaction. Plant J. **39:** 1–12.

Feng, H., Wang, X., Zhang, Q., Fu, Y., Feng, C., Wang, B., Huang, L., and Kang, Z. (2014). Monodehydroascorbate reductase gene, regulated by the wheat PN-2013 miRNA, contributes to adult wheat plant resistance to stripe rust through ROS metabolism. Biochim. Biophys. Acta **1839:** 1–12.

Froehlich, J.E., Benning, C., and Dörmann, P. (2001). The digalactosyldiacylglycerol (DGDG) synthase DGD1 is inserted into the outer envelope membrane of chloroplasts in a manner independent of the general import pathway and does not depend on direct interaction with monogalactosyldiacylglycerol synthase for DGDG biosynthesis. J. Biol. Chem. **276:** 31806–31812.

Fu, D., Uauy, C., Distelfeld, A., Blechl, A., Epstein, L., Chen, X., Sela, H., Fahima, T., and Dubcovsky, J. (2009). A kinase-START gene confers temperature-dependent resistance to wheat stripe rust. Science **323:** 1357–1360.

Greenberg, J.T. (1996). Programmed cell death: a way of life for plants. Proc. Natl. Acad. Sci. USA **93:** 12094–12097.

Hovmøller, M.S., Walter, S., and Justesen, A.F. (2010). Escalating threat of wheat rusts. Science **329:** 369.

Hung, C.Y., Aspesi, P., Jr., Hunter, M.R., Lomax, A.W., and Perera, I.Y. (2014). Phosphoinositide-signaling is one component of a robust plant defense response. Front. Plant Sci. **5:** 267.

Krattinger, S.G., Lagudah, E.S., Spielmeyer, W., Singh, R.P., Huerta-Espino, J., McFadden, H., Bossolini, E., Selter, L.L., and Keller, B. (2009). A putative ABC transporter confers durable resistance to multiple fungal pathogens in wheat. Science **323:** 1360–1363.

Levine, A., Tenhaken, R., Dixon, R., and Lamb, C. (1994). H_2O_2 from the oxidative burst orchestrates the plant hypersensitive disease resistance response. Cell **79:** 583–593.

Li, C., Distelfeld, A., Comis, A., and Dubcovsky, J. (2011). Wheat flowering repressor VRN2 and promoter CO2 compete for interactions with NUCLEAR FACTOR-Y complexes. Plant J. **67:** 763–773.

Loewen, C.J.R., and Levine, T.P. (2005). A highly conserved binding site in vesicle-associated membrane protein-associated protein (VAP) for the FFAT motif of lipid-binding proteins. J. Biol. Chem. **280:** 14097–14104.

Lowe, I., Cantu, D., and Dubcovsky, J. (2011). Durable resistance to the wheat rusts: integrating systems biology and traditional phenotype-based research methods to guide the deployment of resistance genes. Euphytica **179:** 69–79.

Maccaferri, M., Zhang, J., Bulli, P., Abate, Z., Chao, S., Cantu, D., Bossolini, E., Chen, X., Pumphrey, M., and Dubcovsky, J. (2015). A genome-wide association study of resistance to stripe rust (*Puccinia striiformis* f. sp. *tritici*) in a worldwide collection of hexaploid spring wheat (*Triticum aestivum* L.). G3 (Bethesda) **5:** 449–465.

Maruta, T., Tanouchi, A., Tamoi, M., Yabuta, Y., Yoshimura, K., Ishikawa, T., and Shigeoka, S. (2010). Arabidopsis chloroplastic ascorbate peroxidase isoenzymes play a dual role in photoprotection and gene regulation under photooxidative stress. Plant Cell Physiol. **51:** 190–200.

McIntosh, R.A., Yamazaki, Y., Dubcovsky, J., Rogers, W.J., Morris, C.F., Appels, R., and Xia, X.C. (2013). Catalogue of Gene Symbols for Wheat. (http://wheat.pw.usda.gov/GG2/Triticum/wgc/2013/GeneCatalogueIntroduction.pdf).

Michelmore, R.W., Christopoulou, M., and Caldwell, K.S. (2013). Impacts of resistance gene genetics, function, and evolution on a durable future. Annu. Rev. Phytopathol. **51:** 291–319.

Midorikawa, T., and Inoue, K. (2013). Multiple fates of non-mature lumenal proteins in thylakoids. Plant J. **76:** 73–86.

Milus, E.A., Kristensen, K., and Hovmøller, M.S. (2009). Evidence for increased aggressiveness in a recent widespread strain of *Puccinia striiformis* f. sp. *tritici* causing stripe rust of wheat. Phytopathology **99:** 89–94.

Munnik, T., and Vermeer, J.E.M. (2010). Osmotic stress-induced phosphoinositide and inositol phosphate signalling in plants. Plant Cell Environ. **33:** 655–669.

Nakagawa, T., Kurose, T., Hino, T., Tanaka, K., Kawamukai, M., Niwa, Y., Toyooka, K., Matsuoka, K., Jinbo, T., and Kimura, T. (2007). Development of series of gateway binary vectors, pGWBs, for realizing efficient construction of fusion genes for plant transformation. J. Biosci. Bioeng. **104:** 34–41.

Okubara, P.A., Blechl, A.E., McCormick, S.P., Alexander, N.J., Dill-Macky, R., and Hohn, T.M. (2002). Engineering deoxynivalenol metabolism in wheat through the expression of a fungal trichothecene acetyltransferase gene. Theor. Appl. Genet. **106:** 74–83.

Park, J., Gu, Y., Lee, Y., Yang, Z., and Lee, Y. (2004). Phosphatidic acid induces leaf cell death in Arabidopsis by activating the Rho-related small G protein GTPase-mediated pathway of reactive oxygen species generation. Plant Physiol. **134:** 129–136.

Pavet, V., Olmos, E., Kiddle, G., Mowla, S., Kumar, S., Antoniw, J., Alvarez, M.E., and Foyer, C.H. (2005). Ascorbic acid deficiency activates cell death and disease resistance responses in Arabidopsis. Plant Physiol. **139:** 1291–1303.

Radhamony, R.N., and Theg, S.M. (2006). Evidence for an ER to Golgi to chloroplast protein transport pathway. Trends Cell Biol. **16:** 385–387.

Raho, N., Ramirez, L., Lanteri, M.L., Gonorazky, G., Lamattina, L., ten Have, A., and Laxalt, A.M. (2011). Phosphatidic acid production in chitosan-elicited tomato cells, via both phospholipase D and phospholipase C/diacylglycerol kinase, requires nitric oxide. J. Plant Physiol. **168:** 534–539.

Risacher, T., Craze, M., Bowden, S., Paul, W., and Barsby, T. (2009). Highly efficient *Agrobacterium*-mediated transformation of wheat via *in planta* inoculation. In Methods in Molecular Biology: Transgenic Wheat, Barley and Oats, H.D. Jones and P.R. Shewry, eds (New York: Humana Press), pp. 115–124.

Rohila, J.S., et al. (2006). Protein-protein interactions of tandem affinity purification-tagged protein kinases in rice. Plant J. **46:** 1–13.

Sacco, F., Suarez, E.Y., and Naranjo, T. (1998). Mapping of the leaf rust resistance gene *Lr3* on chromosome 6B of Sinvalocho MA wheat. Genome **41:** 686–690.

Schrick, K., Nguyen, D., Karlowski, W.M., and Mayer, K.F.X. (2004). START lipid/sterol-binding domains are amplified in plants and are predominantly associated with homeodomain transcription factors. Genome Biol. **5:** R41.

Schrick, K., Bruno, M., Khosla, A., Cox, P.N., Marlatt, S.A., Roque, R.A., Nguyen, H.C., He, C., Snyder, M.P., Singh, D., and Yadav, G. (2014). Shared functions of plant and mammalian StAR-related lipid transfer (START) domains in modulating transcription factor activity. BMC Biol. **12:** 70.

Shi, L.X., and Theg, S.M. (2013). The chloroplast protein import system: From algae to trees. Biochim. Biophys. Acta **1833:** 314–331.

Shigeoka, S., Ishikawa, T., Tamoi, M., Miyagawa, Y., Takeda, T., Yabuta, Y., and Yoshimura, K. (2002). Regulation and function of ascorbate peroxidase isoenzymes. J. Exp. Bot. **53:** 1305–1319.

Spoel, S.H., and Dong, X. (2012). How do plants achieve immunity? Defence without specialized immune cells. Nat. Rev. Immunol. **12:** 89–100.

Stahl, T., Glockmann, C., Soll, J., and Heins, L. (1999). Tic40, a new "old" subunit of the chloroplast protein import translocon. J. Biol. Chem. **274:** 37467–37472.

Staiger, D., and Brown, J.W.S. (2013). Alternative splicing at the intersection of biological timing, development, and stress responses. Plant Cell **25:** 3640–3656.

Syed, N.H., Kalyna, M., Marquez, Y., Barta, A., and Brown, J.W.S. (2012). Alternative splicing in plants—coming of age. Trends Plant Sci. **17:** 616–623.

Tang, D., Ade, J., Frye, C.A., and Innes, R.W. (2005). Regulation of plant defense responses in Arabidopsis by EDR2, a PH and START domain-containing protein. Plant J. **44:** 245–257.

Testerink, C., and Munnik, T. (2011). Molecular, cellular, and physiological responses to phosphatidic acid formation in plants. J. Exp. Bot. **62:** 2349–2361.

Torres, M.A. (2010). ROS in biotic interactions. Physiol. Plant. **138:** 414–429.

Tripp, J., Inoue, K., Keegstra, K., and Froehlich, J.E. (2007). A novel serine/proline-rich domain in combination with a transmembrane domain is required for the insertion of AtTic40 into the inner envelope membrane of chloroplasts. Plant J. **52:** 824–838.

Vorwerk, S., Schiff, C., Santamaria, M., Koh, S., Nishimura, M., Vogel, J., Somerville, C., and Somerville, S. (2007). *EDR2* negatively regulates salicylic acid-based defenses and cell death during powdery mildew infections of *Arabidopsis thaliana.* BMC Plant Biol. **7:** 35.

Wang, C.F., Huang, L.L., Buchenauer, H., Han, Q.M., Zhang, H.C., and Kang, Z.S. (2007). Histochemical studies on the accumulation of reactive oxygen species (O_2^- and H_2O_2) in the incompatible and compatible interaction of wheat - *Puccinia striiformis* f. sp. *tritici.* Physiol. Mol. Plant Pathol. **71:** 230–239.

Yang, B., Ruan, R., Cantu, D., Wang, X., Ji, W., Ronald, P.C., and Dubcovsky, J. (2013). A comparative approach expands the protein-protein interaction node of the immune receptor *XA21* in wheat and rice. Genome **56:** 315–326.

Supplemental Figures

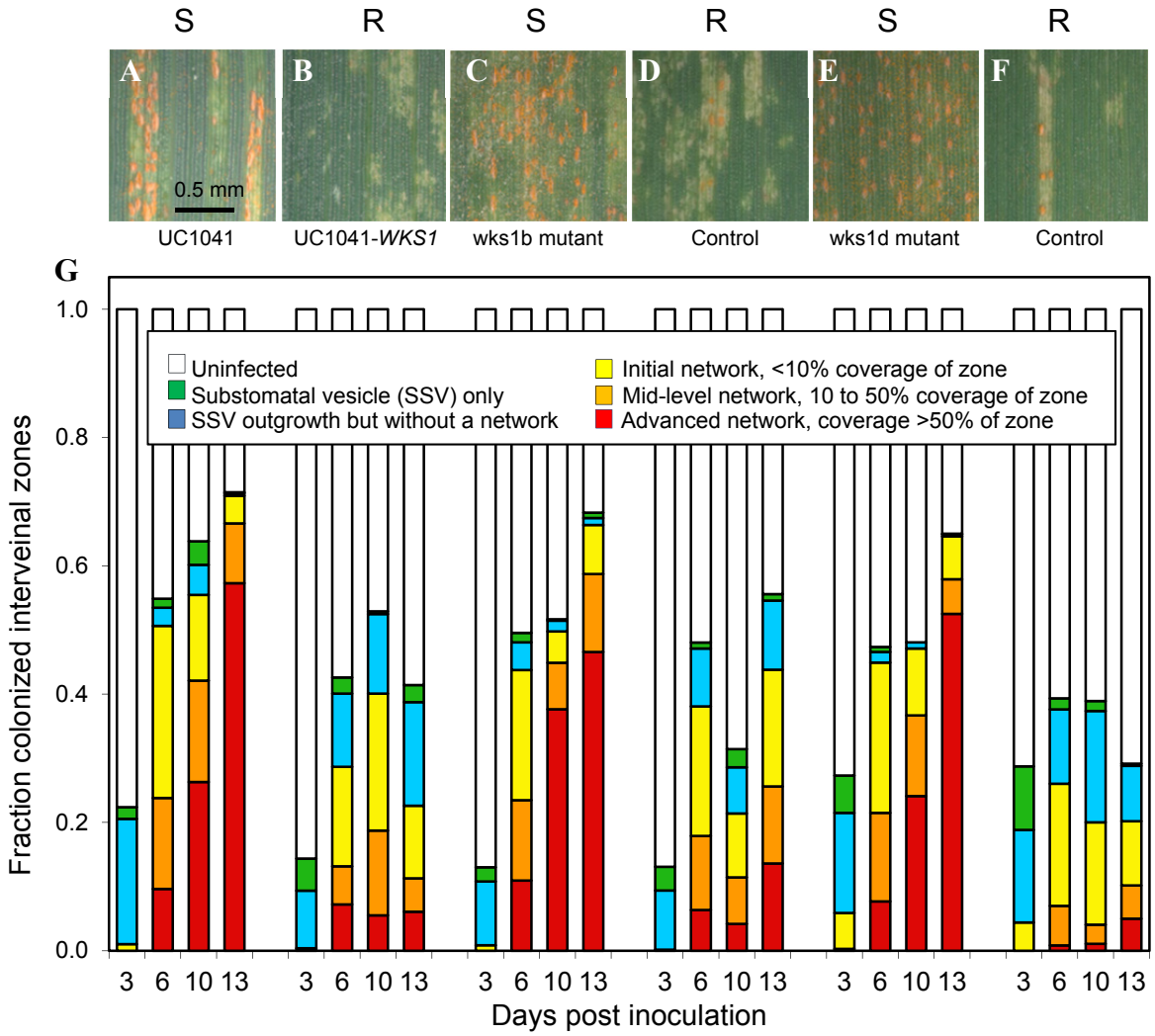

Supplemental Figure 1. Pathogen Growth and Development in Interveinal Regions of Uvitex-Stained Leaves in Three Pairs of Hexaploid Wheat Isogenic Lines With and Without *WKS1*.

(A) UC1041 control (S= susceptible).

(B) UC1041 with wild type *WKS1* (R= resistant).

(C) wks1b susceptible mutant (mutation in kinase domain, Supplemental Figure 3A).

(D) Sister line of wks1b homozygous for wild type *WKS1* (resistant control).

(E) wks1d susceptible mutant (mutation in kinase domain, Supplemental Figure 3A).

(F) Sister line of wks1d homozygous for wild type *WKS1* (resistant control).

(G) Pathogen growth and development in three pairs of isogenic lines with and without *WKS1*. Initial fungal development was similar, including urediniospore germination, germling penetration into stoma, and formation of substomatal vesicles and haustorial mother cells.

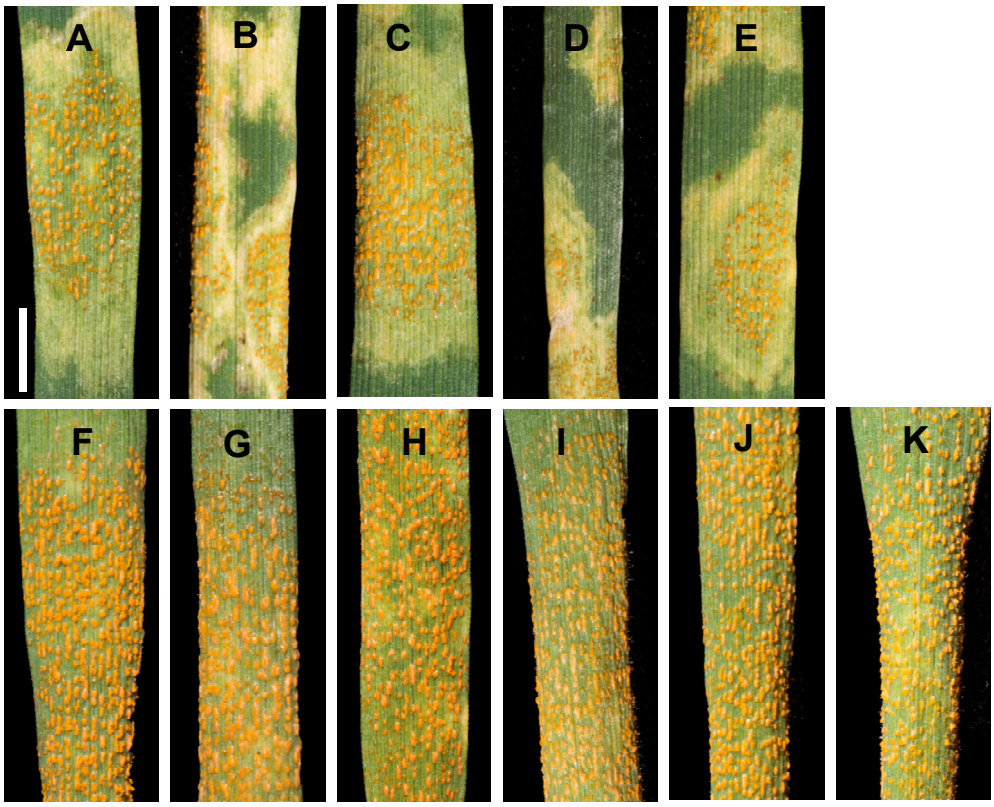

Supplemental Figure 2. Wheat Plants Transformed with NP:WKS1.1 or NP:WKS1.2 and Inoculated with *Pst* Race PST-08/21.

(A-E) NP:WKS1.1 transformed plants, events 1 through 5, respectively
(F-K) NP:WKS1.2 transformed plants, events 1 through 6, respectively.
Each panel shows a representative plant from independent events. Pictures were taken 15 days after inoculation. Scale: 0.5 cm.

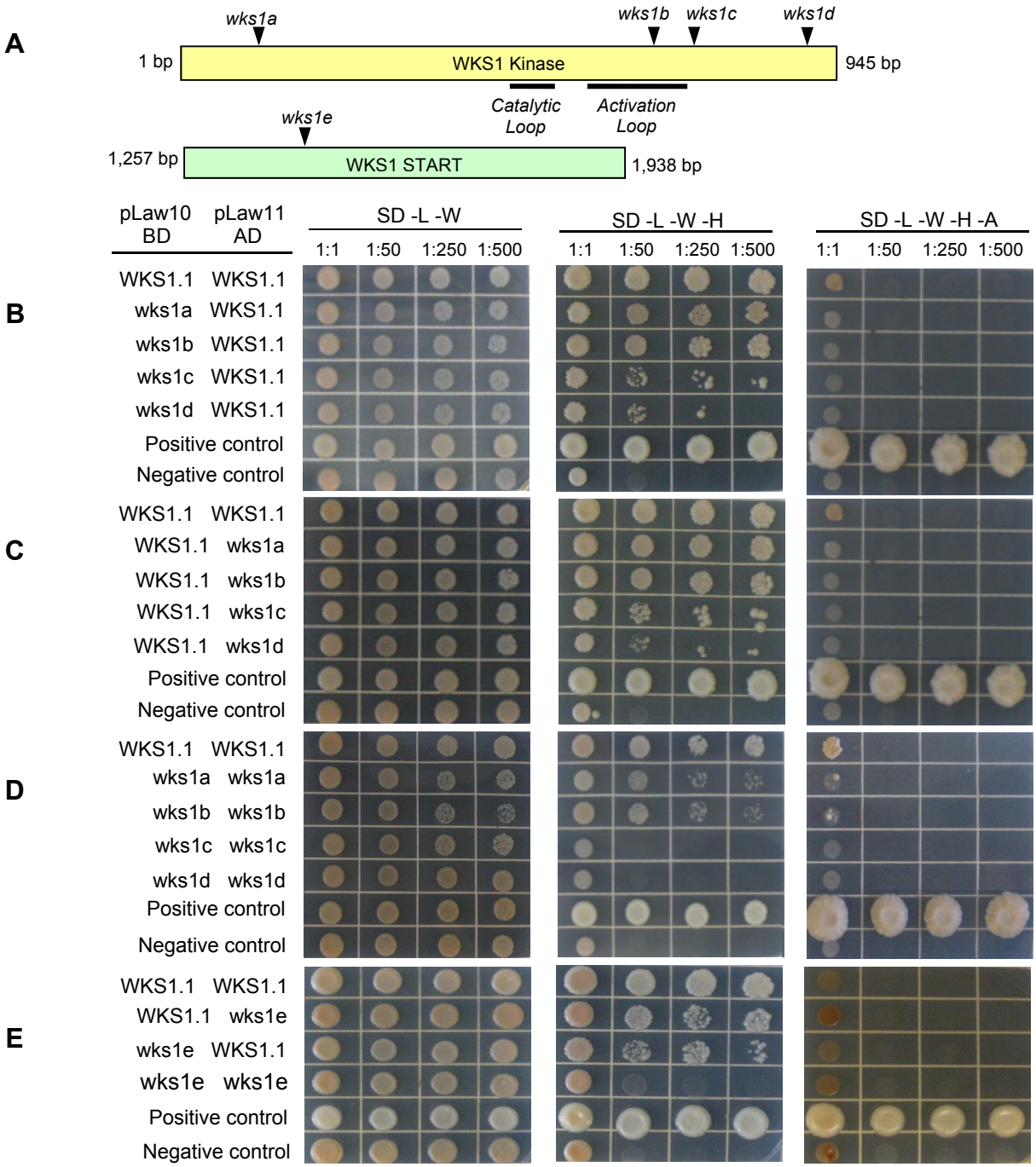

Supplemental Figure 3. Effect of WKS1.1 Mutations on Homodimer Formation.

(A) Location of WKS1.1 point mutations resulting in *Pst* susceptible plants. Numbers to the left and right of each rectangle refer to DNA co-ordinates in the WKS1.1 coding region.
(B-C) Interactions between mutant and wild-type WKS1.1 as activation (B) or binding domain (C).
(D) Homodimerization of wks1a-d kinase-mutants.
(E) Homodimerization of wks1e START-mutant and its interactions with the wild-type WKS1.1.
(B-E) Positive control = pGBKT7-53/pGADT7-T; Negative Control = pLAW10/pLAW11. BD= binding AD= activation domain. See also Supplemental Figure 5 for control Western Blots.

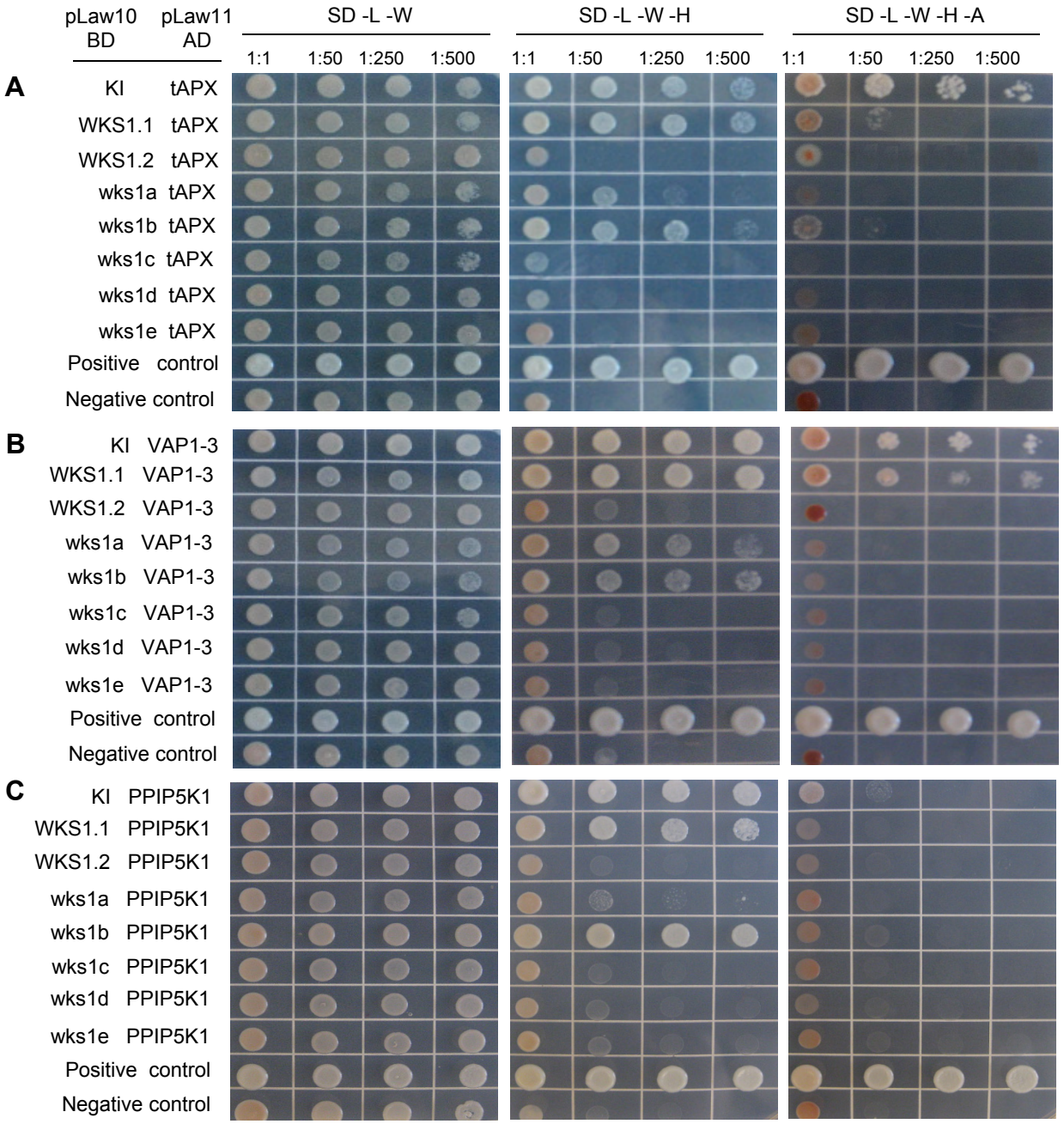

Supplemental Figure 4. Y2H Assays Between WKS1 Variants and Interacting Proteins tAPX, VAP1-3 and PPIP5K1-like.

(A) tAPX (clone identified in the Y2H screen including the last five exons)
(B) VAP1-3 (full length).
(C) PPIP5K1-like (clone identified in the Y2H screen including the last three exons).
(A-C) Positive control = pGBKT7-53/pGADT7-T; Negative Control = pLAW10/pLAW11. See Supplemental Figure 5 for control Western Blots. KI= Kinase-Inter-domain, wks1a-e= mutants.

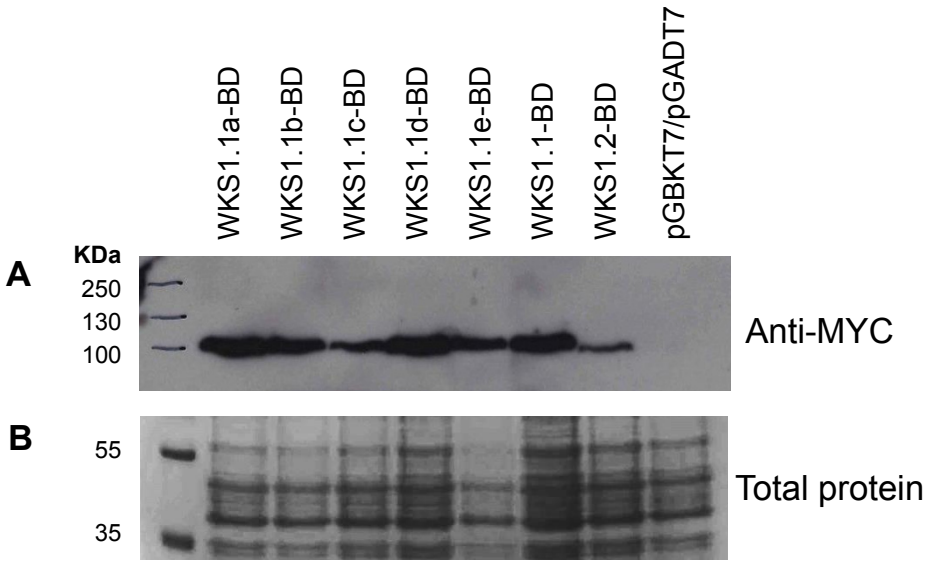

Supplemental Figure 5. Western Blot Confirming that Mutant and Alternative Splice WKS1.2 Proteins Are Not Degraded in Negative Y2H Interactions in Figure 3 and Supplemental Figures 3 and 4.

(A) Western blot detection of mutant and alternative spliced WKS1 proteins using Myc Epitope Tag Antibody (Myc.A7) and a secondary goat anti-rabbit IgG peroxidase conjugate (see Supplemental Method 4). Mutant and alternative spliced WKS1 proteins were not degraded in negative Y2H interactions. BD=binding domain, pGBKT7/pGADT7= negative control.
(B) Total protein included as a loading control.

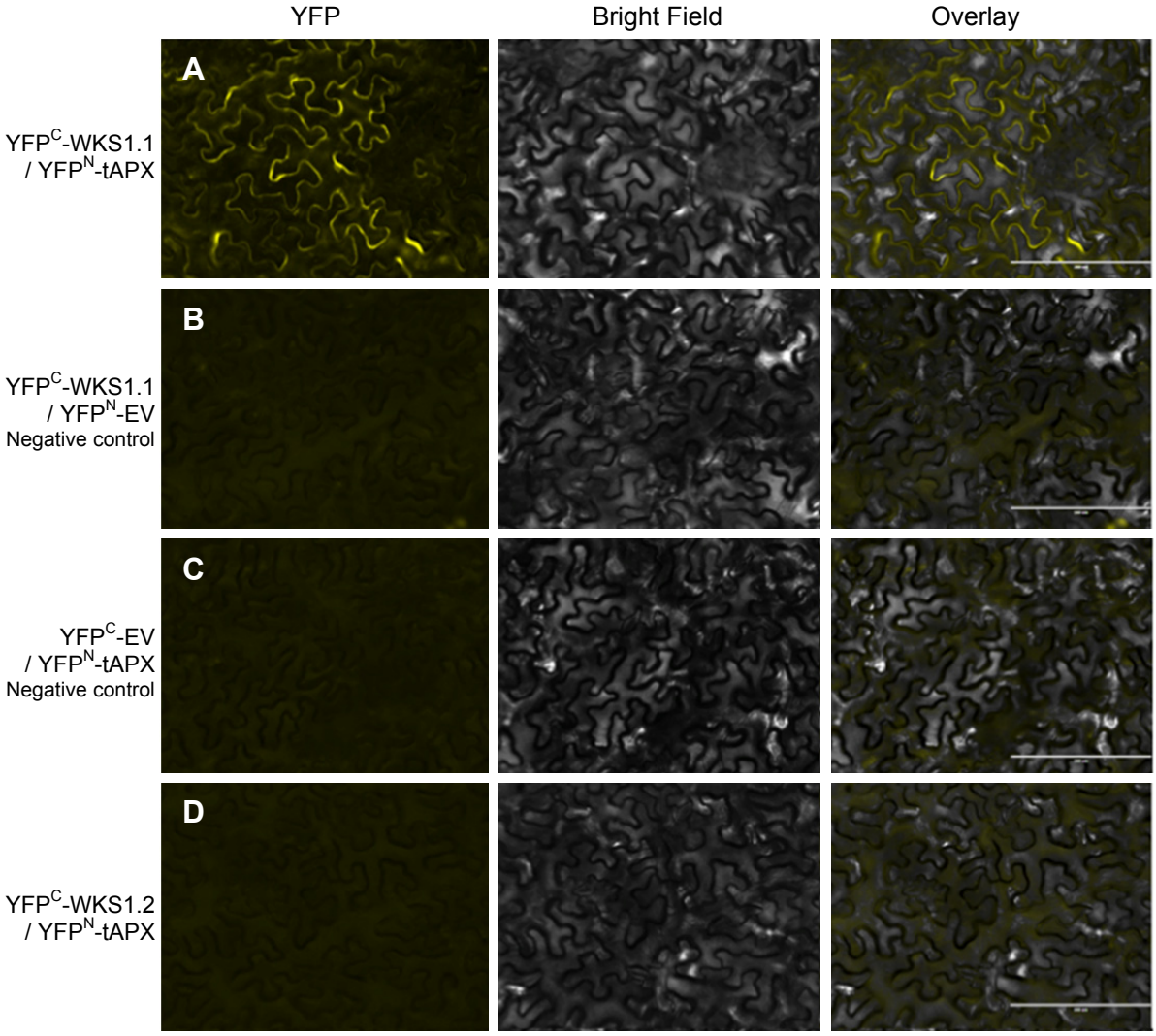

Supplemental Figure 6. Interaction Between tAPX and Splice Variants WKS1.1 and WKS1.2 by Bimolecular Fluorescence Complementation (BiFC).

(A) YFP^C-WKS1.1 and YFP^N-tAPX. YFP= YELLOW FLUORESCENCE PROTEIN, YFP^N= amino-terminal region, YFP^C= carboxy-terminal region, EV= empty vector. White bar indicates 200 µm in all pictures. Transient expression in *Nicotiana benthamiana* leaf epidermal cells followed protocols published before (Chang et al., 2013).

(B) YFP^C-WKS1.1 and YFP^N-EV. Abbreviations and methods are described in panel (A).

(C) YFP^C- EV and YFP^N-tAPX. Abbreviations and methods are described in panel (A).

(D) YFP^C-WKS1.2 and YFP^N-tAPX. Abbreviations and methods are described in panel (A).

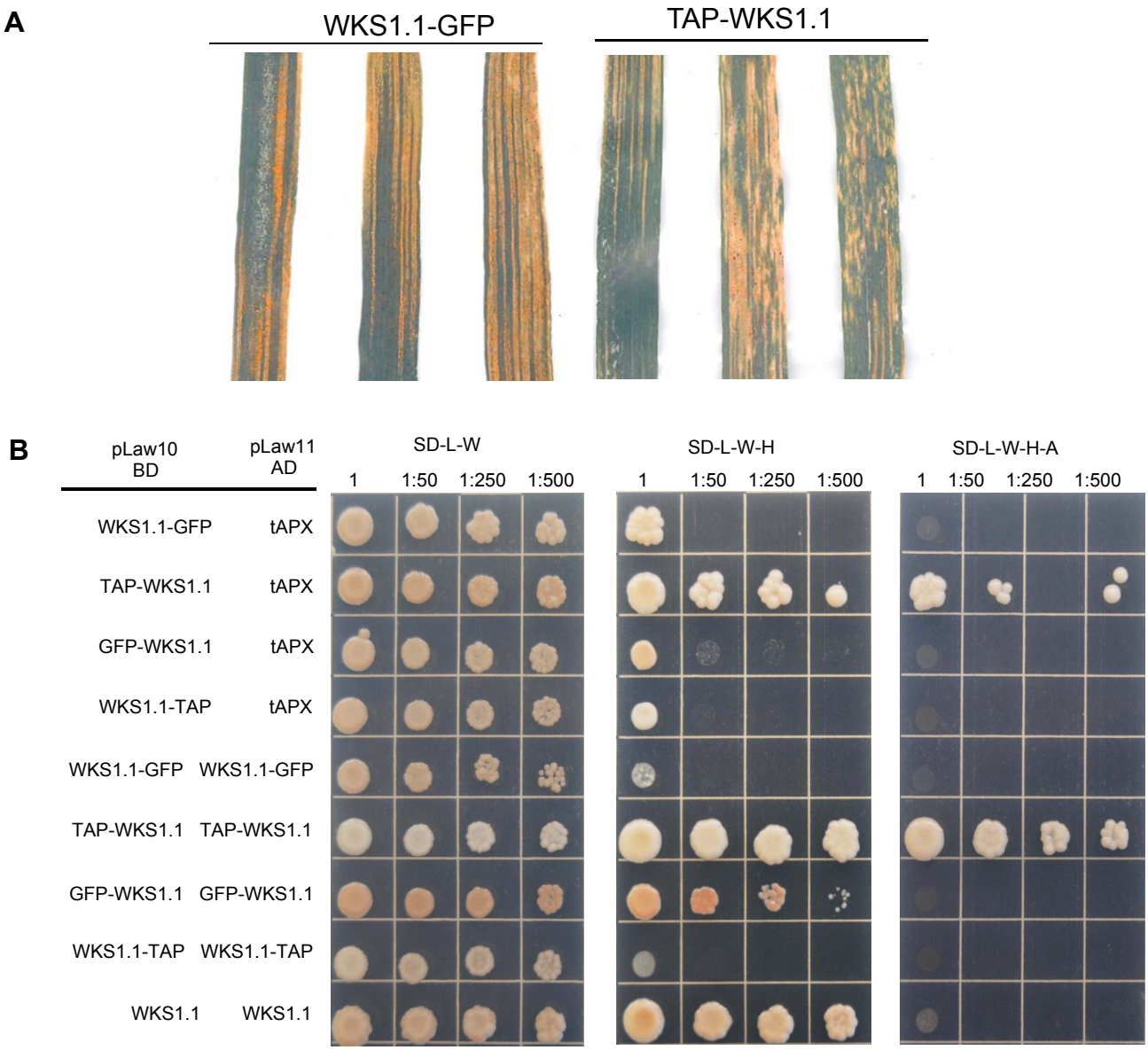

Supplemental Figure 7. Effect of WKS1.1 Fusions with Tags at the N- or C-Terminal Regions on Interactions with Full-length tAPX in Y2H Assays and on Resistance to *Pst*.

(A) Reaction to *Pst* race PST130 in transgenic wheat plants transformed with NP:WKS1.1-GFP (susceptible) and Ubi:TAP-WKS1.1 (partial resistance).

(B) Effect of GFP and TAP tags at the amino- and carboxy-terminus of WKS1.1 on the formation of homodimers and on the interactions with full-length tAPX. None of the constructs showed auto-activation when tested against an empty-bait or -prey vector.

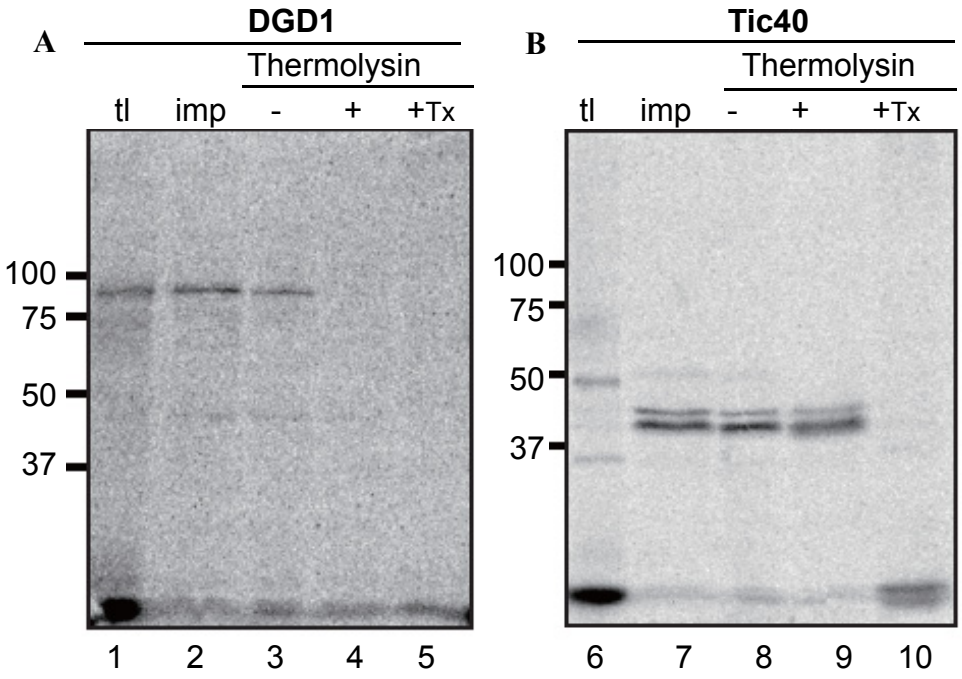

Supplemental Figure 8. Controls for the *in vitro* Chloroplast Import Assays.

(A-B) Radiolabeled DGD1 and Tic40 controls incubated with intact chloroplasts. tl = 10% of translation products, imp. = intact chloroplasts 20 min under import condition, thermolysin = chloroplasts incubated on ice for 30 min without (-) or with (+) thermolysin, or with thermolysin and 2% (v/v) Triton X-100 (Tx). Radiolabeled proteins were visualized using a phosphorimager. The sizes of molecular weight markers in kDa are shown to the left of each image

(A) DGD1 is an outer membrane protein (Froehlich et al., 2001) that is digested by the thermolysin treatment (lane 4).

(B) Tic40 is an inner membrane protein (Stahl et al., 1999) that is resistant to the thermolysin treatment (lane 9).

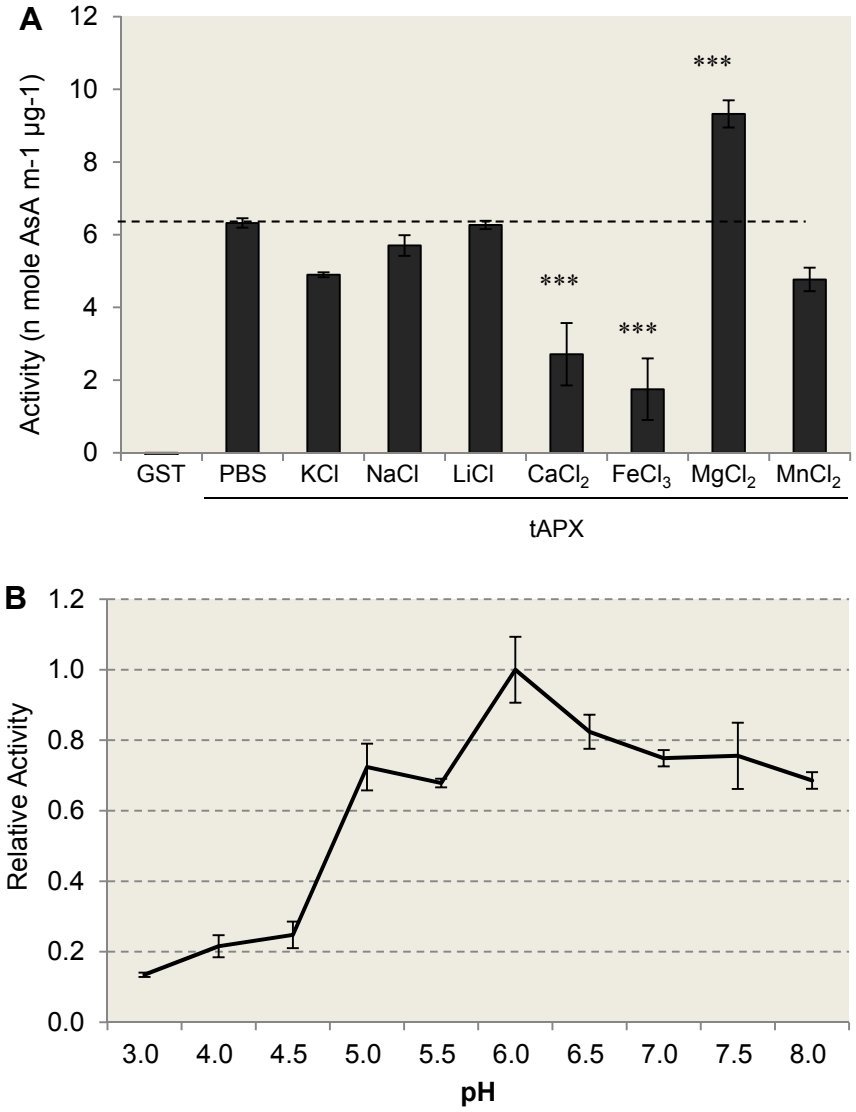

Supplemental Figure 9. Effect of Different Ions and pH on tAPX Activity *in vitro*.

(A) Effect of different ions on tAPX Activity. GST = no tAPX, PBS = indicates control buffer without ions. Concentrations of KCl and NaCl are 50 mM while other ions are at 5 mM (n = 4, *** = $P < 0.001$, Dunnett test vs. PBS control). Error bars indicate standard errors of the means.
(B) Effect of pH on tAPX activity. The specific enzymatic activity at pH6.0 was set as 1. Error bars indicate standard errors of the means (n = 4).

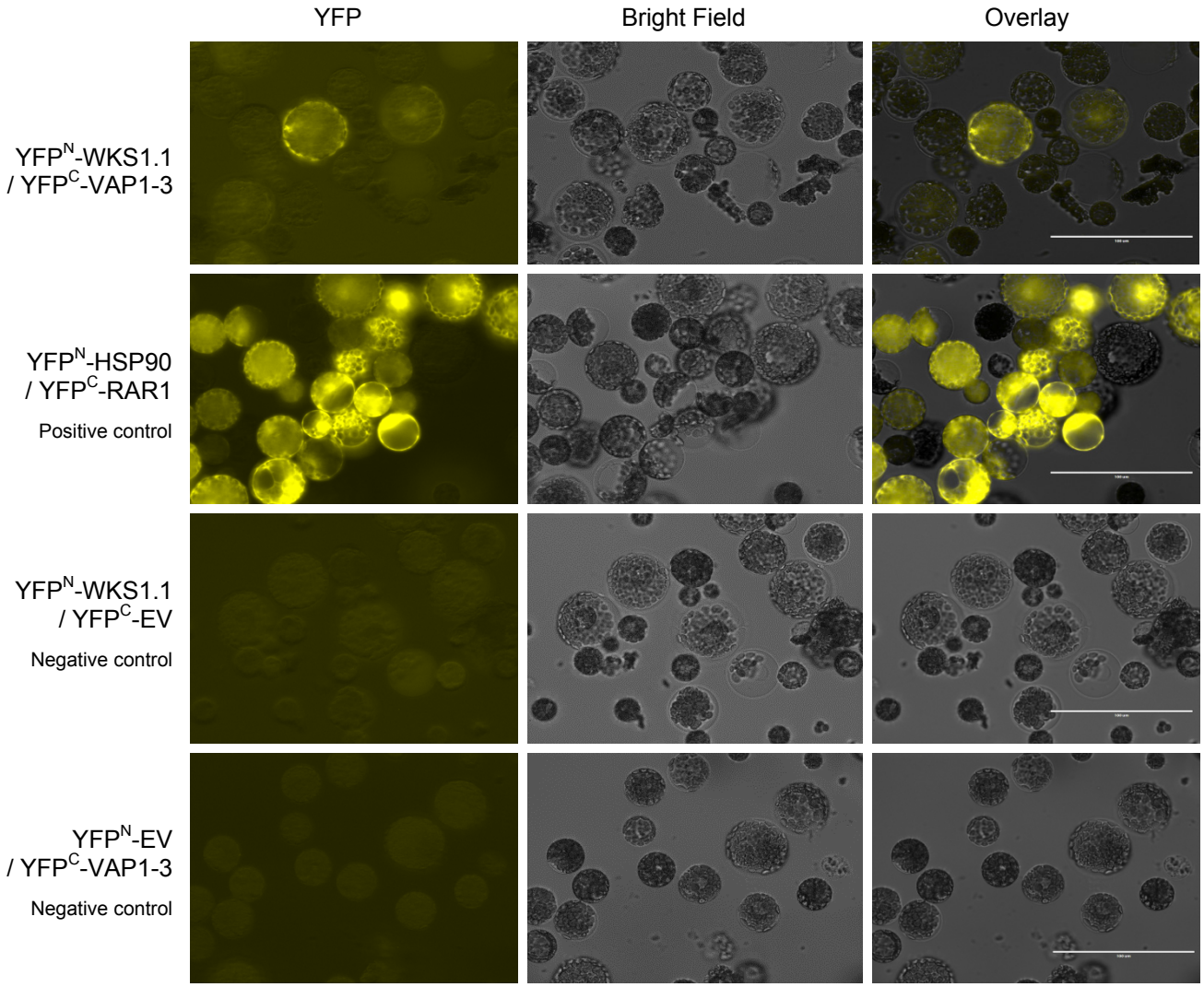

Supplemental Figure 10. Validation of the Interaction between VAP1-3 and WKS1.1 by Bimolecular Fluorescence Complementation (BiFC) in *N. benthamiana* Protoplasts.

YFP= YELLOW FLUORESCENCE PROTEIN, YFP^N= amino-terminal region, YFP^C= carboxy-terminal region. BiFC methods are as described before (Cantu et al., 2013). The positive control shows a stronger interaction between wheat HSP90 and RAR1 (Cantu et al., 2013). Negative controls include VAP1-3 and WKS1.1 combined with empty vector (EV). White bar indicates 100 µm.

Supplemental Tables

Supplemental Table 1. Average Resistance of Plants Transformed with NP:WKS1.1 and NP:WKS1.2 and Inoculated with *Pst* Race PST-08/21.

Background	Line or Event (N[1])		Figure[2]	Infection score[3] ± SE	Comments
Glasgow	Glasgow susceptible control (5)		Fig.1B	4.00 ± 0.00	Abundant sporulation, highly susceptible.
UC1041	UC1041 susceptible control (10)		Fig.1C	3.85 ± 0.10	Abundant sporulation, highly susceptible.
UC1041	UC1041+*WKS1* resistant control (10)		Fig.1D	1.28 ± 0.13	Clearly defined necrotic *Yr36* response, partial res.
Glasgow	NP:WKS1.1	Event 1 (10)	Fig.1F	1.30 ± 0.15	Clearly defined necrotic *Yr36* response, partial res.
		Event 2 (10)	Fig.1G	1.20 ± 0.13	Clearly defined necrotic *Yr36* response, partial res.
		Event 3 (10)	SF2a-e	1.40 ± 0.16	Clearly defined necrotic *Yr36* response, partial res.
		Event 4 (10)	SF2a-e	1.30 ± 0.15	Clearly defined necrotic *Yr36* response, partial res.
		Event 5 (5)	SF2a-e	1.20 ± 0.14	Clearly defined necrotic *Yr36* response, partial res.
Glasgow	NP:WKS1.2	Event 1 (7)	Fig.1E	4.00 ± 0.00	Abundant sporulation, no *Yr36* response, highly susceptible.
		Event 2 (7)	SF2f-k	3.86 ± 0.12	Abundant sporulation, no *Yr36* response, highly susceptible.
		Event 3 (7)	SF2f-k	3.86 ± 0.12	Abundant sporulation, no *Yr36* response, highly susceptible.
		Event 4 (7)	SF2f-k	3.86 ± 0.12	Abundant sporulation, no *Yr36* response, highly susceptible.
		Event 5 (7)	SF2f-k	3.71 ± 0.15	Abundant sporulation, no *Yr36* response, highly susceptible.
		Event 6 (7)	SF2f-k	4.00 ± 0.00	Abundant sporulation, no *Yr36* response, highly susceptible.

[1] Number of plants scored per line or event.
[2] Pictures shown in Figure 1 (Fig.1) or Supplemental Figure 2 (SF2) a-e= WKS1.1, f-k=WKS1.2.
[3] Infection evaluation: 0, no sporulation; 1, light sporulation; 2, intermediate sporulation; 3, moderate sporulation; 4, abundant sporulation.

Supplemental Table 2. Primers Used in This Study**.**

Primer Name	Primer Sequence	Objective
GST-WKS1 F	GCGGAATTCATGGAGCTCCCACGAAACAA	GST-WKS1.1 fusion
GST-WKS1.1 R	GCGCTCGAGTCAACTTTCACCACTTCCTG	
GST-WKS1 F	GCGGAATTCATGGAGCTCCCACGAAACAA	GST-WKS1.2 fusion
GST-WKS1.2 R	GCGCTCGAGTTAATTGTGGTATCTTGCAA	
ATG_F	CACCATGGAGCTCCCACGAAACAAAC	WKS1.1 clone for Y2H
Full_R	TCAACTTTCACCACTTCCTGA	
ATG_F	CACCATGGAGCTCCCACGAAACAAAC	WKS1.2 clone for Y2H
WKS1.2_R	GAGACTAGGACACATAACATTAATTG	
ATG_F	CACCATGGAGCTCCCACGAAACAAAC	WKS1 Kinase alone (KA) for Y2H
Kinase_R	AAGACGTTCTACAACATGATTCA	
ATG_F	CACCATGGAGCTCCCACGAAACAAAC	WKS1 Kinase + inter-domain (KI) for Y2H
KI_R	ATCATATGTCGTTCCCACAGGTC	
IS_F	CACCATGCGAATGCTTGGTAAAGATCAC	WKS1 Inter-domain + START (IS) for Y2H
Full_R	TCAACTTTCACCACTTCCTGA	
START_F	CACCATGTGGCGTCTTCTCGGATGCCAGAA	WKS1 START alone (SA) for Y2H
Full_R	TCAACTTTCACCACTTCCTGA	
TILL_569_F	GTGCCTTTGGTGAG**A**TTTTCCGAGGTTTTC	*wks1a* mutant (V55I) for Y2H
TILL_569_R	CTTTGCCAACATGAGTTCTATAGTTCTTAG	
TILL_312_F	CTAATAATGTAATA**A**GAAGCAGAGGTTAC	*wks1b* mutant (G199R) for Y2H
TILL_312_R	TAAAATAACTATTCTCCATAGAAAGCAACC	
TILL_480_F	AGAACACATTCAGA**T**TGGCCGGGTTGATC	*wks1c* mutant (T211I) for Y2H
TILL_480_R	GGATCCATGTAACCTCTGCTTCCTATTACA	
TILL_138_F	GGATATCAAGAAAC**A**TCCTGAAATGAATC	*wks1d* mutant (R205H) for Y2H
TILL_138_R	CTTCTGAGACACTCAATTGCCAGCTCTCC	
TILL_567_F	TATGAGTGG**A**ACTGCAGCTTCTCGT	*wks1e* mutant (D477N) for Y2H
TILL_567_R	ACGGCTACTGTCCATGCTCATGAGA	
UbiP-F1	TTTAGCCCTGCCTTCATACG	Validation of transgenic Ubi:NTAP-WKS1.1
TAP-F95	TCATCCAGAGCCTGAAGGAC	
TAP-R254	TTCAGGTTTGGGAGATGGAG	
START-pTNT-F	GCGGGTACCATGTGGCGTCTTCTCGGATGCCAGAA	Cloning START domain into GST-START for chloroplast import assay
WKS1R	GCGCCCGGGTCAACTTTCACCACTTCCTG	
tAPX-6B-F tAPC-6B-R	GCATTCTTGACGTCTCTGGTC CATCTTGCATGCCGACCAAT	Marker for the deletion of tAPX in chromosome arm 6BL
tAPX-BamH1-F	cgg*GGATCC*ATGGCGGCGTCGGAGGCCGCGCA	Recombinant tAPX protein purification for activity assay
tAPX-Xho1-R	cgg*CTCGAG*TTAGTTCCCGGCCAGAGACGTCAAG	

Supplemental Table 2. Continuation.

Primer Name	Primer Sequence	Objective
WKS1.1EcoRIF	cc*GAATTC*TATGGAGCTCCCACGAAACAA	Clone WKS1.1 kinase and kinase-linker into pET41b
WKS1.1KR	gtg*CTCGAG*AAGACGTTCTACAACATGATTCAT	
WKS1.1KIRXhoI	gtg*CTCGAG*TATGTCGTTCCCACAGGTCCAATC	
WKS1-for	GTACCATGGAGCTCCCACGAAACAA	Cloning of WKS1.1 and WKS1.2
WKS1.1-rev	AAAGCGCGCTACGTATCAACTTTCACCACTTCCTG	
WKS1.2-rev	AAAGCGCGCTACGTATCAATTGTGGTATCTTGCAA	
VAP1-3_F	CACCGAGGAAGCCACCATGAG	Full length VAP1-3 interactor
VAP1-3_R	CTACTCTTCTCCTATGTCTTCTTGA	
tAPX_F	ccATGGCGGAGCGCATCG	Full length tAPX interactor into pET28a
tAPX_R	CCTGGAAAATGGTTAATTACA	
PPIP5K-like_UF1	caCCCGTGGGCAGATCGG	Full length PPIP5K-like interactor into pENTRY
PPIP5K-like_SR1	GTTGCCACCAAATGTTAACAAAG	

All primers are written from 5' to 3' end. Start codons are underlined in the forward primers and stop codons are underlined in the reverse primers. For the five *wks1* mutant alleles generated by inverse-PCR the base changed in each allele is in bold and underlined in the forward primer. The amino acid change generated by each mutation and its position in the protein is indicated in parentheses. Lower case letters in the primers indicate added nucleotides to increase restriction efficiency

Supplemental Table 3. WKS1 Protein Interactors Detected in Y2H Screen and Their Y2H Interactions with Alternative Splice Variants WKS1.1 and WKS1.2 and Mutants (wks1a-e).

Closest plant protein	Thylakoid-associated ascorbate peroxidase	Vesicle-associated protein 1-3-like	Inositol hexakisphosphate & diphosphoinositol-pentakisphosphate kinase 1-like
Proposed abbreviation	tAPX	VAP1-3	PPIP5K1-like
GenBank accession	KJ614568	KJ614569	KJ614570
# of clones identified in Y2H	3 (2 FL, 1 KI) [1]	2 (KI) [1]	1 (KI) [1]
Validation	Full-length	Full-length	Partial (last 3 exons)
KI	Y	Y	Y
WKS1.1	Y	Y	Y
WKS1.2	N	N	N
wks1a	Y	Y	N
wks1b	Y	Y	Y
wks1c	N	N	N
wks1d	N	N	N
wks1e	N	N	N

[1] FL indicates clones detected with the full length WKS1.1 and KI clones detected with the Kinase + inter-domain region. Y = positive interaction and N = no interaction.

Supplemental Methods

Supplemental Method 1. Time Course of *Pst* Infection.

Six-week-old plants were inoculated with *Pst* as described before (Fu et al., 2009), harvested after 3, 6, 10 and 13 days, and fixed and stained in uvitex (Moldenhauer et al., 2006). One cm^2 leaf segments were evaluated with a Nikon Microphot SA fluorescence microscope with a UV-2A DM 400 filter (Nikon, Melville, NY, USA). Because *Pst* infections are limited by the parallel veins in the mature wheat leaves, fungal development in different interveinal zones generally arise from independent infection events. Interveinal zones in each of three different leaves from four replicates per time point were evaluated. Development of fungal growth in each inter-veinal zone in each leaf segment was recorded as either uninfected, only sub-stomatal vesicles, sub-stomatal vesicles with hyphal outgrowth but no fungal network, and different levels of fungal network development: < 10% ("initial network"), 10-50% ("mid-level network") and >50% (advanced network") of the inter-veinal zone. Formation of an extensive network in the mesophyll precedes the formation of the uredinia, which gives rise to the urediniospores.

Supplemental Method 2. Transgenic Lines.

NP:WKS1.1 and NP:WKS1.2 in Glasgow: NP:WKS1.1 and NP:WKS1.2 were initially cloned into the Entry vector pENTR/d-TOPO (Invitrogen, UK) without stop codons. Stop codons were incorporated by amplifying the WKS1.1 and WKS1.2 3' terminal regions with stop codon sequences included into the reverse primers, and replacing the respective *Spe*I-*Bss*HII fragments. NP:WKS1.1-stop and NP:WKS1.2-stop were then digested with *Not*I and *Sna*BI, and 5' termini filled in with T4 polymerase, prior to ligation into the *Pme*I site of binary vector pRLF10. The *A.tumefaciens* supervirulent strain EHA105 (Hood et al., 1993) was used for transformation of the T-DNAs into immature Glasgow wheat embryos using protocols described before (Risacher et al., 2009). Plantlets were transferred to Jiffy-7 peat pellets, and, following analysis by quantitative PCR for the copy number of the nptII gene, potted on, vernalized, and grown to maturity. Stable homozygous lines were identified by PCR and segregation ratio; phenotypic analysis was performed on T_4 plants. For stripe rust inoculation plants were infected at 10°C and kept 24 hour in dark and high humidity conditions. Afterwards, plants were transferred to a control environment room (CER) with a 19-14°C day/night temperature cycle (16h light/8h dark).

Ubi:TAP-WKS1.1 in Bobwhite: WKS1.1 was initially cloned into the Entry vector pENTR/d-TOPO (Invitrogen, Grace Island, NY, USA) and then incorporated into a Gateway binary destination vector Ubi-NTAP-1300 kindly provided by Michael Fromm (Rohila et al., 2006). Calluses derived from immature embryos of hexaploid spring variety Bobwhite were bombarded using a 1:1 molar ratio of Ubi:TAP-WKS1.1 and Ubi:BAR selectable marker plasmids (15.5 µg total) coated onto 1000 nm gold particles (Seashell Technology, La Jolla, CA, USA), according to the manufacturer's instructions. Transformants were selected as described before (Fu et al., 2009). Independent transgenic T_1 lines were obtained and positive plants were confirmed by PCR using primer pair TAP-F95 and TAP-R254 or by Western Blot

using TAP tag polyclonal antibody (Pierce, Thermo Fisher Scientific Inc. Rockford, IL). Phenotypic analysis was performed in T_3 and T_4 transgenic plants.

NP:WKS1.1-GFP in Bobwhite: Stable transgenic plants were generated in the spring wheat variety Bobwhite by bombardments using the same procedure described above (Table 1). Two independent transgenic events were generated with a construct encoding a fusion protein between WKS1.1 and GFP under the regulation of the 3.5 kb promoter region of WKS1 (NP:WKS1.1-GFP). As a control we developed an additional transgenic plant expressing GFP under the regulation of the same promoter region (NP:GFP) (Table 1). The presence of the GFP transgene was verified by PCR.

Fluorescence microscopy was performed using an Olympus FV1000 confocal laser scanning microscope (MCB LM Imaging Facility, Department of Molecular & Cellular Biology, University of California, Davis). For GFP the excitation wavelength was 488 nm and emission was 500 to 535 nm and for chlorophyll the excitation wavelength was 633 nm and emission was 645 to 745 nm.

Supplemental Method 3. *In vitro* Lipid Binding Assays.

To express the GST-fused WKS1.1 and WKS1.2 proteins in wheat germ extracts, we first cloned the two GST fusions into the pGEX-6P-1 vector (GE Healthcare Bio-Sciences, Pittsburgh, PA, USA) between the *Eco*R1 and *Xho*I sites (primers are described in Supplemental Table 1). The resulting pGEX clones were then subcloned into the pTNT vector (Promega, Madison, WI, USA) which was used for *in vitro* synthesis of protein using wheat germ extracts. To generate the pTNT GST-START$_{WKS1.1}$ clone, the START domain of WKS1.1 (without inter-domain region) was directly subcloned into the pTNT vector by using the START $_{WKS1.1}$ pTNT F and WKS1R primers (Supplemental Table 1), which contain an *Acc65*I site and *Xma*I site, respectively.

For the *in vitro* mRNA synthesis, the two pTNT plasmids were linearized with *Bgl*II. The plasmids constructs were then purified and transcribed *in vitro* using the Ribomax-T7 RNA production system (Promega, Madison, WI, USA). After extraction with phenol/chloroform/isoamyl alcohol (25:24:1) and chloroform/isoamyl alcohol (24:1), the mRNA was precipitated and washed with ethanol, dissolved in RNase-free water and stored at -80 ºC. The quality and quantity of the mRNA was determined by using Nanodrop (Thermo Fisher, Wilmington, DE, USA).

For the *in vitro* protein synthesis we used the wheat germ system following the manufacturers' instructions (Promega, Madison, WI USA). Expressed proteins were purified on GST SpinTrap purification columns (GE Healthcare, Piscataway, NJ, USA). Eluted proteins were dialyzed overnight in phosphate buffered saline (PBS) to remove glutathione and quantified by employing the BCA protein assay reagent (Pierce, Rockford, IL, USA). A 15 µl aliquot from the wheat germ reactions was combined with 3 µl of NuPAGE (Invitrogen, Grace Island, NY, USA) sample buffer, boiled for 3 min and separated by Nupage 4-12% Bis-Tris polyacrylamide gel electrophoresis prior to blotting onto nitrocellulose membranes (Bio-

Rad, Richmond, CA, USA) for immunoblots. Immunoblots on nitrocellulose were blocked with 5% nonfat milk in PBST (PBS with 0.05% Tween 20) for 1 h and washed in PBST.

For the lipid binding assays lipid strips and phosphatidylinositol (PIP) strips (Echelon Biosciences, Salt Lake City, UT USA) were blocked for 1 h with PBST, containing 3% (w/v) fatty acid free BSA. All subsequent incubations and washes included PBST/3% BSA. Membranes were incubated overnight at 4^{o} C with 9 µg/mL of each of the GST fusions separately, then washed four times over 45 min, and incubated for 2 h with rabbit anti-GST (Millipore, Billerica, MA, USA) at a 1:4,000 dilution. Membranes were then washed, incubated with anti-rabbit IgG-HRP at 1:10,000 dilution, and washed again before developing with SuperSignal West Pico Chemiluminescence substrate (Pierce Protein Biology Systems, Thermo Scientific, Rockford, IL, USA) and imaged using a Kodak Image Station 2000RT (Eastman Kodak, Rochester, NY, USA).

Supplemental Method 4. Yeast Two-hybrid (Y2H) Assays.

Bait/prey co-transformants generated by the lithium acetate method (Gietz and Woods, 2002) were selected on solid SD agar medium lacking leucine (L) and tryptophan (W). Positive transformants were then re-plated on SD medium lacking L, W, histidine (H) and adenine (A) to test for interaction. Three dilutions of 1:50, 1:250, and 1:500 were compared. pLAW10 and pLAW11 empty vectors were used as negative controls. A bait vector containing murine p53 (pGBKT7-53) and prey vector containing SV-40 large T-antigen (pGADT7-T) provided in the Matchmaker kit (Clontech Laboratories, Mountain View, CA, USA) were used as positive interaction controls. Auto-activation was tested by co-transforming bait and prey constructs with their reciprocal empty vector. Five point mutations previously shown to abolish WKS1 resistance (Fu et al., 2009) were introduced in the Y2H full length WKS1 construct using primers described in Supplemental Table 1 and the Phusion Site-Directed Mutagenesis kit (New England Biolabs, Ipswich, MA, USA). Full length WKS1 and WKS1 truncation constructs were cloned using primers described in Supplemental Table 1 and integrated into Y2H bait (pLAW10) and prey (pLAW11) vector backbones via Gateway recombination.

To test if the negative Y2H interactions of the WKS1.1 mutants and WKS1.2 were caused by the degradation of the modified WKS1 proteins, we co-transformed tAPX-plaw11 with WKS1.1a-, WKS1.1b-, WKS1.1c-, WKS1.1d-, WKS1.1e-, WKS1.1- or WKS1.2-plaw10 respectively into yeast AH109 gold. Total protein was extracted and approximately 20 µg protein was loaded in each lane. Proteins were detected in Western blots using a 1:1000 dilution of primary antibody against Myc Epitope Tag (Myc.A7, Thermo Scientific Catalog#: MA1-21316), and a 1:5000 dilution of goat anti-mouse IgG peroxidase conjugate secondary antibody (EMD Millipore's Calbiochem ® Billerica MA USA, catalogue # DC02L).

Supplemental Method 5. Wheat cDNA Y2H Library Screening and Validation.

We screened a cDNA Y2H library previously generated using RNA extracted from leaves of tetraploid wheat *Triticum turgidum* L. ssp. *durum* cv. Langdon infected with *Puccinia striiformis* race PST113 (Yang

et al., 2013). The library was cloned into prey vector pGADT7-Rec and transformed into strain Y187 (*MATα*). The compatible mating strain, Y2H Gold (*MAT*a), was transformed with pLAW10 bait vector containing either the full-length WKS1 or the kinase with the inter-domain region (KI). Mating procedures followed Matchmaker Gold Yeast Two-Hybrid System protocols (Clontech Laboratories, Mountain View, CA, USA). The mated library was initially plated on solid SD -L -W -H media, after which positive colonies were collected and transferred onto SD -L -W -H -A plates for more stringent selection. Plasmid DNA was extracted from positive yeast colonies using the QIAprep Spin Miniprep Kit (Qiagen, Redwood, City, CA, USA) and amplified in *E. coli* before sequencing using the Matchmaker AD LD-Insert Screening Amplimer Set (Clontech). To test for auto-activation, purified prey plasmids were co-transformed with empty bait vector, and were also re-transformed with the original bait construct to validate the positive growth obtained in the library screen.

Supplemental Method 6. *In vitro* Chloroplast Localization.

Radiolabeled precursors of WKS1.1 and WKS1.1-START domain (without any tag) were prepared using the TNT® T7 Coupled Wheat germ System (Promega, Madison, WI, USA) and L-[35S]-methionine (Amersham Biosciences, Piscataway, NJ, USA). Chloroplasts were prepared from pea seedlings grown in the greenhouse (Bruce et al., 1994). *In vitro* mRNA synthesis and protein synthesis were carried out using the TnT SP6 coupled reticulocyte lysate system (Promega, Madison, WI USA) followed the original manufacturers' instructions and was done on a 400 µl scale. After TnT reaction, radiolabeled proteins were incubated with isolated chloroplasts under light for 20 min, and then chloroplasts were re-isolated using 40% Percoll. After import for 20 min*, the reaction mixture was divided into four fractions. Intact chloroplasts in each fraction were re-isolated by a 40% Percoll cushion. The first fraction was saved as total import (imp).

Three other samples were resuspended to 0.5 µg chlorophyll/µL in import buffer containing 10 mM CaCl2 without (mock), or with 0.2 µg/µL thermolysin (+ t-lysin), or with 0.2 µg/µL thermolysin and 2 % Triton X-100 (+ t-lysin & TX100). After incubation for 30 min on ice, the protease activity was quenched by addition of EDTA to a final concentration of 10 mM. Chloroplasts were then re-isolated thorough a 40% Percoll Cushion containing 10 mM EDTA and resuspended in 100 µL of import buffer. Chlorohyll concentration of each sample was quantified by measuring absorbance at 652 nm and a sample containing 5 µg chlorophylls was loaded onto each lane.

For the time course of WKS1.1 *in vitro* chloroplast import assay, each reaction contained isolated chloroplasts (12.5 µg chlorophyll), 10 µL of the translation product and 3 mM Mg-ATP in import buffer. After incubation at room temperature under light, intact chloroplasts were re-isolated at different time points using 40% Percoll and were directly loaded onto 10% SDS-PAGE. The radiolabeled proteins were visualized by phosphor-imager analysis. Two Arabidopsis proteins, DGD1 and Tic40, were included as technical controls. Arabidopsis transcription factor DGD1 (Gabriele et al., 2010) is not transported into the

chloroplast (Figure 4C) and chloroplast inner envelope membrane translocon complex protein Tic40 is transported into chloroplast (Figure 4D) and is located in the stroma (Chou et al., 2003).

The presence of a chloroplast localization signal in WKS1 was tested using prediction programs ChloroP (http://www.cbs.dtu.dk/services/ChloroP/), iPSORT (http://ipsort.hgc.jp/) , Predotar (https://urgi.versailles.inra.fr/predotar/predotar.html), and TargetP (http://www.cbs.dtu.dk/services/TargetP/).

Supplemental Method 7. Co-immunoprecipitation (CoIP).

For the WKS1-tAPX CoIP experiment, the supernatant of a total protein extract from leaves of Ubi:TAP-WKS1.1 transgenic plants was mixed with 100–150 µl of IgG Sepharose beads (Amersham Biosciences, Piscataway, NJ, USA) and incubated at 4 ºC for 1 h with continuous rotation. After centrifugation at 200 g for 2–3 min, IgG supernatant was discarded and the collected IgG beads were washed in 30 ml extraction buffer lacking protease inhibitors. The washed beads were loaded onto a disposable chromatography column and washed with 10 ml Tobacco Etch Virus (TEV) cleavage buffer (10 mM Tris–HCl pH 8.0, 150 mM NaCl, 0.1% IGEPAL, 0.5 mM EDTA, 1 mM DTT). The TAP-tagged proteins were released by digestion with 30 µl TEV protease (300-500 U; Invitrogen) in TEV cleavage buffer containing 1 l M E-64 protease inhibitor for 1 h at 16 C. The TEV cleaved eluate was adjusted to 2 mM $CaCl_2$ and diluted in 3 volumes of calmodulin binding buffer (CBB: 10 mM b-mercaptoethanol; 10 mM Tris–HCl pH 8.0; 150 mM NaCl; 1 mM Mg-acetate; 1 mM imidazole; 2 mM $CaCl_2$; 0.1% IGEPAL) and incubated with 100 µl of calmodulin-agarose beads (Stratagene, La Jolla, CA, USA) for 1 h at 4 °C. The calmodulin-agarose beads were washed in 30 ml of calmodulin binding buffer and the proteins were eluted with buffer containing 10 mM beta -mercaptoethanol, 10 mM Tris–HCl pH 8.0, 150 mM NaCl, 1 mM Mgacetate, 1 mM imidazole, 2 mM EGTA, 0.1% IGEPAL. The eluted proteins were precipitated with trichloroacetic acid and loaded onto a 4-15% gradient polyacrylamide gel for SDS-PAGE. After SDS-PAGE the proteins were transferred to a nitrocellulose membrane for Western blot, employing tAPX-specific antibodies (Agrisera, Vännäs, Sweden).

Supplemental Method 8. Recombinant WKS1-Kinase, tAPX and PPIP5K1-like Protein Purification.

The pET41b plasmids including the WKS1-kinase domain (KA) and the full-length *tAPX* and *PPIP5K1-like* genes were transformed into BL21 (DE3) plysS competent cells (Promega, Madison, WI USA). Bacteria was grown in TB medium to OD600 0.6~0.8 first at 37 °C and then at 25 °C before induction with 0.5 mM IPTG overnight. The cells were collected and suspended in 1/10 volume of B-PER Bacterial Protein Extraction Reagent (Pierce, Thermo Fisher Scientific Inc. Rockford, IL, USA) with Complete Mini Protease Inhibitor Cocktail Tablets (Roche Diagnostics Corporation, Indianapolis, IN, USA). The cells were sonicated three times each for 30 s and incubated for 1 h with shaking in ice. After centrifugation at 18,000 rpm for 1 h, the supernatant was removed to a new tube, adjusted to 100 mM HEPES pH7.4, 500 mM NaCl, 1 mM ASA, 20 mM imidazole and mixed with 0.5 ml pre-equilibrated Ni-NTA resin (Pierce

Biotechnology Inc., Rockford, IL, USA) for 1 h in ice. The samples were then loaded into columns and washed with 20 volumes of binding buffer. Recombinant protein was mixed with 1 ml of Elution Buffer (100mM HEPES pH7.4, 500 mM NaCl, 1 mM ASA, 250 mM imidazole, 10% glycerol), held for 10 min, and then eluted. The protein was dialyzed overnight against dialysis buffer (100mM HEPES pH7.4, 500 mM NaCl, 1 mM ASA, 10% glycerol). Protein concentration was quantified with Qubit Protein Assay Kits (Molecular Probes, Life Technologies Corporation, Grand Island, NY, USA).

Supplemental Method 9. Phosphorylation Assays.

For the phospho-fluorescence assay, the reactions including 2 µg of each recombinant protein were stopped by adding 4 volumes of cold acetone and kept at -20 °C overnight. The proteins were pelleted by centrifugation at 15,000 rpm for 15 minutes and air-dried. Dried proteins were suspended in 200 µl of Pro-Q Diamond Phosphoprotein Gel Stain (Molecular Probes ®, Life Tech. Grand Island, NY USA) in the dark for 1 h at room temperature. Proteins were pelleted again with cold acetone and washed three more times to remove the residual stain. Stained proteins were suspended in 200 µl of ddH_2O to quantify the fluorescence using a Tecan (Life Technologies, Grand Island, NY, USA) plate reader (excitation= 488 nm and emission= 595 nm).

For the *in vitro* phosphorylation assay, 5µl of γ-^{32}P-ATP (NEG502A001MC, 3000 Ci/mmol, 10mCi/ml, PerkinElmer Inc. Waltham, MA, USA) was mixed with 1 µg of WKS1.1 kinase protein and 5 µg of tAPX or PPIP5K1-like (control) recombinant protein in a kinase reaction buffer and kept for 30 minutes at room temperature. The samples were passed through a 7KMWCO Zeba Spin desalting column (Pierce, Thermo Fisher Scientific Inc. Rockford, IL) to remove the remaining free ATP. The samples were then separated in 10% SDS-PAGE and exposed to a phosphor-imager overnight. The IP image was collected with FUJI Film FIA-9000 (Suzhou, China).

For the *in vitro* and *in planta* gel retardation assays, ¼ volume of Laemmli Protein Loading Buffer Pack (Fermentas, Thermo Fisher Scientific Inc. Rockford, IL) was added to the samples, which were then boiled for 5 min. Protein samples were loaded onto 14% SDS PAGE with100 µM acrylamide-pendant Phos-tag and 100 µM of $MnCl_2$ (Wako Pure Chemical Industries, Ltd.). The proteins were run at 60 volts overnight in a 4 °C cold room. The gels were washed with 1 mM EDTA twice to remove the residual Mn^{2+} and twice with transfer buffer before electronic transfer and Western Blot detection with rabbit anti-tAPX antibody (Agrisera, Vännäs, Sweden, catalog number AS08 368).

Supplemental Method 10. tAPX Activity Assays.

tAPX Activity *in vitro* Assay: The recombinants tAPX protein was purified as described in Supplemental Method 8. For the activity assay, 2 µg of recombinant WKS1-KA protein was mixed with tAPX reaction buffer (50 mM PBS, 1 mM ascorbic acid, 10 mM $MgCl_2$ or other ions), to a total volume of 200 µl. Two µl of 1M H_2O_2 was added to start the reaction, and reads were taken at 290 nm every minute for 20 minutes

at room temperature. Activity was determined based on the absorbance decrease of L-ascorbate at 290 nm (using a standard curve for a linear range L-ascorbate measured also at 290 nm).

tAPX Activity *in planta* Assay: APX activity in wheat plants was measured in 2nd leaves from 6-week old plants. Tissue was ground into fine powder in liquid nitrogen and was mixed with 1.5 ml of extraction buffer (50 mM PBS pH7.0, 40 mM KCl, 10 mM $MgCl_2$, 1 mM AsA, 1% proteinase inhibitor, 1% phosphatase inhibitor and 1 mM PMSF) for 2 minutes at 60Hz in a high through-put grinder (Shanghai Wonhong Biotech Co. Ltd, Shanghai, China). Samples were filtered through miracloth (Millipore) into another 1.5 ml tube to remove cell wall debris. After centrifugation at 300 g for 10 m at 4°C, supernatants were transferred into 1.5 ml tubes and saved as “soluble fraction”. Pellets including the thylakoid fraction were washed thoroughly two times with 0.5 ml extraction buffer, suspended in 0.5 ml extraction buffer and saved as “thylakoid fraction”. To measure APX activity, 50 µl of soluble or thylakoid fractions were mixed with 1.95 ml reaction buffer (50 mMPBS pH7.0, 10 mM $MgCl_2$ and 0.5 mM AsA). Absorbance at 290 nm was measured for 0 minute with a spectrophotometer. 2 µl of 1 M H_2O_2 was added to start the reaction at room temperature and the samples were measured again at 5 minutes. APX activities were calculated based on the decrease of absorbance at 290 nm using a standard curve built with pure ascorbic acid. Four different plants per genotype were used as biological replicates. Protein amounts were determined using a BCA Protein Quantification Kit (Yeasen, Shanghai, China).

SUPPLEMENTAL REFERENCES

Bruce, B.D., Perry, S., Froelich, J., and Keegstra, K. (1994). In vitro import of proteins into chloroplasts. Plant Mol. Biol. Manual **J1:** 1-15.

Cantu, D., Yang, B., Ruan, R., Li, K., Menzo, V., Fu, D., Chern, M., Ronald, P.C., and Dubcovsky, J. (2013). Comparative analysis of the defense response interactomes of rice and wheat BMC Genomics **14:** 166.

Chang, C., Yu, D.S., Jiao, J., Jing, S.J., Schulze-Lefert, P., and Shen, Q.H. (2013). Barley MLA immune receptors directly interfere with antagonistically acting transcription factors to initiate disease resistance signaling. Plant Cell **25:** 1158-1173.

Chou, M.L., Fitzpatrick, L.M., Tu, S.L., Budziszewski, G., Potter-Lewis, S., Akita, M., Levin, J.Z., Keegstra, K., and Li, H.M. (2003). Tic40, a membrane-anchored co-chaperone homolog in the chloroplast protein translocon. EMBO J. **22:** 2970-2980.

Froehlich, J.E., Benning, C., and Dormann, P. (2001). The digalactosyldiacylglycerol (DGDG) synthase DGD1 is inserted into the outer envelope membrane of chloroplasts in a manner independent of the general import pathway and does not depend on direct interaction with monogalactosyldiacylglycerol synthase for DGDG biosynthesis. J. Biol. Chem. **276:** 31806-31812.

Fu, D., Uauy, C., Distelfeld, A., Blechl, A., Epstein, L., Chen, X., Sela, H., Fahima, T., and Dubcovsky, J. (2009). A kinase-START gene confers temperature-dependent resistance to wheat stripe rust. Science **323:** 1357-1360.

Gabriele, S., Rizza, A., Martone, J., Circelli, P., Costantino, P., and Vittorioso, P. (2010). The Dof protein DAG1 mediates PIL5 activity on seed germination by negatively regulating GA biosynthetic gene AtGA3ox1. Plant J. **61:** 312-323.

Gietz, R.D., and Woods, R.A. (2002). Transformation of yeast by lithium acetate/single-stranded carrier DNA/polyethylene glycol method. Method Enzymol **350:** 87-96.

Hood, E.E., Gelvin, S.B., Melchers, L.S., and Hoekema, A. (1993). New *Agrobacterium* helper plasmids for gene-transfer to plants. Transgenic Res. **2:** 208-218.

Moldenhauer, J., Moerschbacher, B.M., and van der Westhuizen, A.J. (2006). Histological investigation of stripe rust (*Puccinia striiformis* f. sp. *tritici*) development in resistant and susceptible wheat cultivars. Plant Pathol. **55:** 469-474.

Risacher, T., Craze, M., Bowden, S., Paul, W., and Barsby, T. (2009). Highly efficient *Agrobacterium*-mediated transformation of wheat via *in planta* inoculation. In Methods in molecular biology. Transgenic wheat, barley and oats, H.D. Jones and P.R. Shewry, eds (New York: Humana Press), pp. 115-124.

Rohila, J.S., Chen, M., Chen, S., Chen, J., Cerny, R., Dardick, C., Canlas, P., Xu, X., Gribskov, M., Kanrar, S., Zhu, J.K., Ronald, P., and Fromm, M.E. (2006). Protein-protein interactions of tandem affinity purification-tagged protein kinases in rice. Plant J. **46:** 1-13.

Stahl, T., Glockmann, C., Soll, J., and Heins, L. (1999). Tic40, a new "old" subunit of the chloroplast protein import translocon. J. Biol. Chem. **274:** 37467-37472.

Yang, B., Ruan, R., Cantu, D., Wang, X., Ji, W., Ronald, P.C., and Dubcovsky, J. (2013). A comparative approach expands the protein-protein interaction node of the immune receptor *XA21* in wheat and rice. Genome **56:** 315-326.